

Heat integrated distillation in a plate packing HiDiC
Master Thesis Project

Theo Krikken
January 24, 2011

Report number: P&E 2433
Student number: 1386603
Chemical Engineering

Delft University of Technology
Faculty 3mE
Process & Energy Department
Intensified Reaction & Separation Systems

Supervisors:
Prof. dr. ir. A.I. Stankiewicz
Dr. Sc. Ž. Olujić
Prof. ir. J. Grievink
Ir. S.A. Tromp

Preface

This report is written for my graduation project at the Process & Energy laboratory of the Delft University of Technology in collaboration with the Energy research Centre of the Netherlands (ECN). The study is part of a large project on the heat integrated distillation column (HIDiC).

First of all I want to thank my supervisor Sander Tromp for his great help and never ending enthusiasm. I also want to thank Žarko Olujić for sharing his limitless knowledge on distillation and structured packing. I learned a lot during the project.

Summary

The heat integrated distillation column (HIDiC) was introduced to improve the energy efficiency of a distillation column. In a HIDiC column the rectifying section is separated from the stripping section of the column, and it is operated at a substantially higher pressure. Because of the higher pressure, condensation in the rectifying section takes place at a higher temperature and when the rectifying section is placed inside or besides the stripping section, heat exchange between the rectifying and stripping section is possible. This results in heating in all stages of the stripping section and cooling in all stages of the rectifying section.

There are two design options for a HIDiC considered in the HIDiC project. The first option is a concentric tray HIDiC in which the rectifying section is placed inside the stripping section. This way, heat can be directly transferred through the wall between the inner and the outer column. The second option, on which the experimental setup is based, is a structured HIDiC. The structured HIDiC is based on the design of a heat exchanger in which stripping sections and rectifying sections are placed alternately, so a rectifying section can exchange heat with the two stripping sections next to it.

The experimental setup as employed in present study simulates one half of a Plate Packing HIDiC, the distillation part can be cooled or heated to simulate operation of a rectifying section or a stripping section of a structured HIDiC respectively. The distillation part consists of two plates of 1000x200 mm with each 5 200x200x7 mm plates of Mellapak 350Y mounted on it in zigzag configuration. The two plates are mounted together with the two layers mirrored towards each other with a perforated plate in between.

Experiments with a mixture of cyclohexane and n-heptane resulted in an average Height Equivalent of a Theoretical Plate (HETP) of 33 cm. In comparison with the earlier tested PF-HIDiC mass transfer in the PP-HIDiC has improved by a factor 4.

Mass transfer was more efficient at higher F-factors, due to a better distribution of liquid over the column and enhanced contact between liquid and vapour.

Heat transfer did have an effect on mass transfer, in stripping mode mass transfer was better than in rectifying mode, but the effect was small and the average separation of the stripping mode and the rectification mode was similar to the separation found in adiabatic operation.

Mass transfer in the partial reboiler was estimated with a set of equations to be able determine the mass transfer in the PP-HIDiC separately from the reboiler. A set of measurements where the flow through the reboiler was changed confirmed the estimations of the separation in the reboiler.

The pressure drop shows a trend as expected from a structured packing column. The experimental pressure drop shows a clear loading and preloading region, with the loading point located at $1.9\text{Pa}^{0.5}$.

The Delft model predicts after shifting the loading point from $1.7\text{Pa}^{0.5}$ to $1.84\text{Pa}^{0.5}$ a similar pressure drop as measured. In the preloading regime the predicted pressure drop is lower than the experimental pressure drop. The higher experimental pressure drop in the preloading section can be declared by the large amount of channels which end at the column wall. The vapour is prevented to flow upwards by wall wipers and therefore has to make a sharp turn into the flow channels directed upwardly, creating extra pressure drop.

The Delft model suggests that the column operates as a column with a completely wetted surface area of $170 \text{ m}^2/\text{m}^3$ while $614 \text{ m}^2/\text{m}^3$ is installed. This shows that about 28% of the surface area is used. Because a metal sheet is installed between the packing plates, triangular channels are formed. The liquid now collects in the lower corners of these channels leaving parts of the surface area unused. In the HiDiC column a lot of these triangular channels end at the column wall, which makes it difficult for both liquid and gas to enter these channels. Due to the inserted plate there are no contact points of crossing channels where in a conventional packed bed liquid tends to mix with liquid flowing through a neighbouring channel in opposite direction. Also the large scale mixing which occurs at transitions between subsequent packing elements is greatly reduced (very limited mixing is in both situations possible through the perforations) by the perforated plate. A PP-HiDiC column with the same packing tightly packed but without the perforated plate could perform better than the current column.

In the HiDiC column heat was transferred from or to the thermal bath fluid. The average UA value in this case was 335 W/K . With a total wall area of 0.4 m^2 the overall heat transfer coefficient U will be $844 \text{ W/m}^2\text{K}$.

List of symbols

A	area	[m ²]
a _e	effective area	[m ² /m ³]
b	corrugation base	[m]
C _p	specific heat	[J/kg K]
d	thickness	[m]
D	diffusion coefficient	[m ² /s]
F	F-factor	[Pa ^{0.5}]
F _{load}	Loading poing	[Pa ^{0.5}]
h	height	[m]
HETP	Height Equivalent of a Theoretical Plate	[m]
HTU	Height of a Transfer Unit	[m]
k	mass transfer coefficient	[m/s]
L	molar liquid stream	[mol/hr]
M	Mass stream	[kg/hr]
N	number of equilibrium stages	[-]
n	number (amount of)	[-]
P_i^{sat}	saturated vapour pressure	[mbar]
Q	amount of heat	[W]
s	corrugation side	[m]
T	Temperature	[°C]
U	overall heat transfer coefficient	[W/m ² K]
u _g	superficial gas velocity	[m/s]
V	molar vapour stream	[mol/hr]
x	liquid composition	[mol/mol]
y	vapour composition	[mol/mol]

Greek

α	relative volatility	[-]
α	incline angle of the packing	[°]
β	crimp angle	[°]
γ	activity coefficient	[
Δ	difference	[-]
Δp	pressure drop	[mbar]
ΔH_{vap}	heat of vaporisation	[J/kg]
ε	porosity of the packing	[-]
λ	stripping factor	[-]
λ_{wall}	heat transfer coefficient of the wall	[W/m K]
μ	viscosity	[Pa s]
ρ	density	[kg/m ³]
σ	surface tension	[N/m]
ϕ	part of a flow channel that is covered by liquid	[-]

Subscript

av	average
adiabatic	adiabatic
b	bottom
ch	cyclohexane
cor	corrugation of a packing plate
column	column
d	distillate
diabatic	diabatic
DC	direction change
exp	experimental
Fenske	calculated with the Fenske equation
g	gas
GL	gas-liquid
GG	gas-gas
l	liquid
nh	n-heptane
packedbed	packed bed
pe	packing element
r	reboiler
reflux	reflux
subcooling	sub cooling

List of abbreviations

dPi	pressure difference
ECN	Energy research Centre of the Netherlands
HETP	Height Equivalent of a Theoretical Plate
HIDiC	Heat Integrated Distillation Column
PF	Plate-Fin
PP	Plate-Packing
VRC	Vapour Recompression Column

Table of Contents

Preface.....	III
Summary.....	IV
List of symbols.....	VI
Table of Contents.....	VIII
1. Introduction.....	1
1.1 What is Distillation?.....	1
1.2 Vapour Recompression distillation Columns.....	2
1.3 Heat Integrated Distillation Column (HIDiC).....	2
1.4 Experimental Setup.....	4
1.5 Goals of this research.....	5
2. Theory.....	6
2.1 Separation performance: the Fenske equation.....	6
2.2 Reboiler stage calculation.....	6
2.3 HETP.....	8
2.4 F-factor.....	9
2.5 Flooding.....	9
2.6 Delft model.....	10
2.6.1 Pressure drop in the Delft model.....	11
2.6.2 Mass transfer in the Delft model.....	11
2.8 Maldistribution.....	12
3. Experimental.....	13
3.1 Experimental setup.....	13
3.2 Column internals.....	14
3.3 Pressure drop.....	15
3.4 Internal reflux.....	15
3.5 Delta T calculations.....	15
3.6 F-factor calculation.....	16
3.7 Delft model.....	16
3.8 Heat transfer.....	18
3.9 Relative volatility.....	19
3.10 Properties of the mixture.....	20
3.11 Analysing the samples.....	20
4. Results and discussion.....	21
4.1 Mass transfer.....	21
4.2 Pressure drop.....	22
4.3 Reboiler stage calculation.....	24
4.4 Heat transfer.....	25
4.5 Maldistribution.....	28
5. Conclusions.....	30
5.1 Mass transfer.....	30
5.2 Pressure drop.....	30
5.3 Heat transfer.....	30
5.4 Maldistribution.....	30
6. Recommendations.....	31
References.....	32
Appendix A: P&ID.....	a
Appendix B: Experimental Data.....	b
Appendix C: Relative volatility.....	e
Appendix D: Reboiler stages.....	f

1. Introduction

Mankind has made use of separation processes for millennia. Early civilizations developed techniques to extract metals from ores¹ and the ancient Mesopotamians were able to extract essential oils from plants for use in perfumes.²

Distillation is one of those very old separation techniques. It goes back to the 5th century BC and was then used for desalination of seawater by Greek sailors³. Distillation led to the discovery of alcohol when the water cooled Morenkop came in use⁴. Now, distillation is the most widely used separation technology in refinery and chemical industry.

1.1 What is Distillation?

Distillation is a separation technique that makes use of the difference in volatility of the components in a mixture. It is a relatively simple technique which is used to separate mixtures into mole fractions or even pure components. Distillation is however an energy intensive separation method. In a distillation column heat required for separation is introduced at a high temperature in the reboiler at the bottom and removed at a low temperature in the condenser at the top. To reach high purities, large reflux streams are needed inside the column to increase the efficiency of the distillation column. A large reflux stream through the column will result in even larger reboiler and condenser duties. About 40% of the energy used in the chemical and refinery industries is associated with separation by distillation⁵, which is 5-6% of the total energy use of mankind.⁶ Because distillation is such an energy intensive process and because it is widely used, there is a high potential for energy savings.

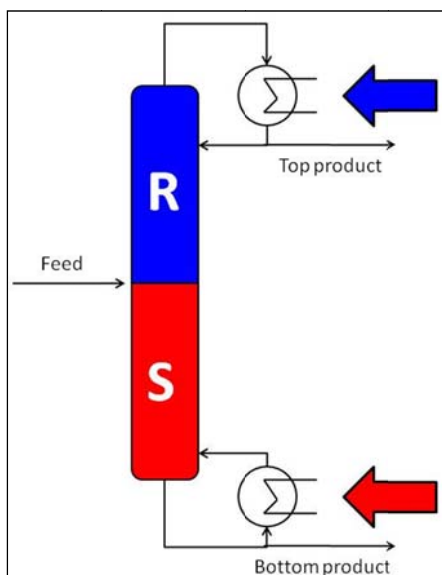


Figure 1 A traditional distillation column¹⁶

1.2 Vapour Recompression distillation Columns

In a conventional distillation column high quality heat is added in the reboiler and low quality heat is removed from the condenser. In fact high quality heat is converted to low quality heat in a distillation column. This low quality heat has little or no use and therefore a distillation column is exergetically very inefficient. To improve the exergetic efficiency of a distillation column, it can be designed as a Vapour Recompression Column (VRC). In a VRC the low quality heat from the condenser is upgraded to high quality heat, so it can be used in the reboiler. This is done by a heat pump, which is in fact a compressor that increases the pressure of the vapour before it enters the condenser/reboiler. In the VRC the vapour stream leaving the top of the column is compressed until the temperature is higher than the temperature required in the reboiler so the vapour can be condensed in one side of the heat exchanger, releasing heat, which is used to evaporate the liquid leaving the bottom of the column on the other side of the heat exchanger. This means the condenser is integrated with the reboiler and the only energy added to the VRC is compression energy. A VRC is only profitable if the temperature difference over the column is sufficiently small, because of the high compressor costs.

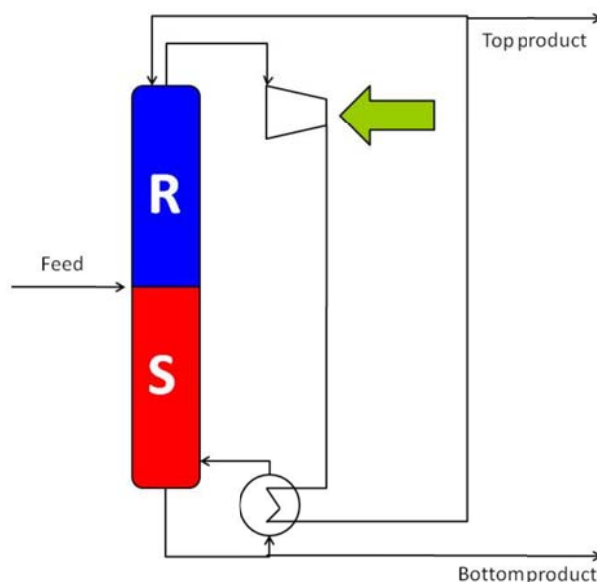


Figure 2 Schematic representation of a Vapour recompression Column.¹⁶

1.3 Heat Integrated Distillation Column (HIDiC)

The main disadvantage of a VRC is the relative high compression ratio that is needed to overcome the temperature difference of the whole column. The use of a VRC is therefore limited to close boiling mixtures.

To make the system of the VRC usable for wider boiling mixtures the Heat Integrated Distillation Column (HIDiC) is developed. A HIDiC is basically a VRC. The main difference is that in a HIDiC column the vapour leaving the stripping section is compressed to the desired level and the whole rectification section is operated at a substantially higher pressure i.e. temperature than in the stripping section. Instead of integrating the condenser and reboiler only, like in a VRC, now the whole rectifying section can be placed inside or besides the stripping section. This causes heating in all stages of the stripping section and cooling in all

stages of the rectifying section. By tuning the energy content of the feed it is even possible to obtain an ideal HIDiC⁹, which means no condenser and reboiler are required. The main advantage of the HIDiC over the VRC is that the compression ratio can be much lower, because only half of the temperature difference of the column has to be overcome.

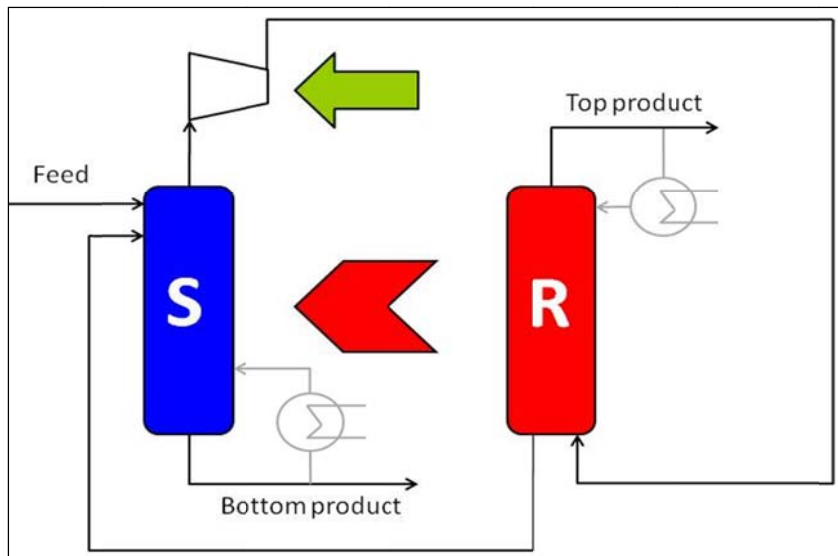


Figure 3 Schematic representation of a HIDiC column¹⁶.

The HIDiC concept is not new. It was introduced by Mah et al⁷ in 1977 and further developed by Aso⁸ and Nakaiwa⁹ in Japan, and by TU Delft¹⁰ and ECN¹¹ in the Netherlands.

In the HIDiC project of TU Delft and ECN there are two different approaches to test the HIDiC concept. One is a concentric HIDiC which consists of an inner and an outer column, in which the inner column is the rectifying section, operated at a higher pressure than the outer column, which is the stripping section. This way, heat can be directly transferred through the wall between the inner and the outer column. The inner and outer column of the pilot plant HIDiC at TU Delft are operated separately, no compressor is installed. They both have their own condenser and reboiler.

Another approach is the use of a (plate fin or plate packing) heat exchanger as a distillation column. In this setup the stripping section and the pressurized rectifying section are alternately placed in the heat exchanger, as shown in Figure 4. This way heat can be transferred through both walls of the heat exchanger from a rectifying section to the two adjacent stripping sections.

1.4 Experimental Setup

The experimental setup used in current work is based on the second option, the heat exchanger based Plate Fin (PF) or Plate Packing (PP) HiDiC. As shown in Figure 4 a stripping section is surrounded by two rectifying sections which are operated at a higher temperature. Heat exchange between the stripping and rectifying section is therefore possible through the walls.

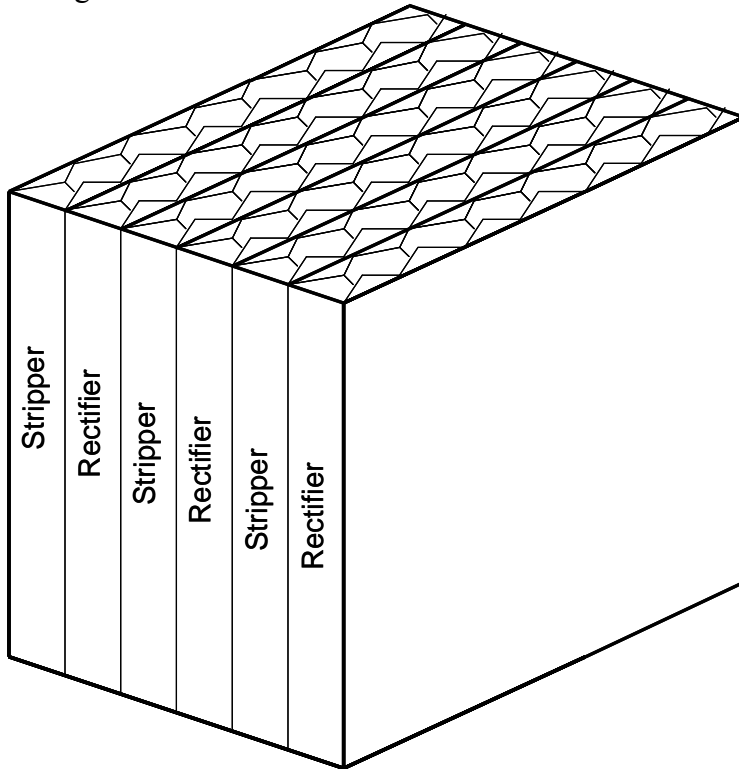


Figure 4 Schematic representation of a PP-HiDiC.

The experimental setup, shown in Figure 5, is in fact one half of a PP-HiDiC with cooling or heating liquid running through double walled plates. This makes it possible to operate the column adiabatically (no cooling or heating), simulate operation of a stripping section (by heating) or a rectification section of a PP-HiDiC (by cooling).

As shown in Figure 5, the rectangular test column has two sample points, one in the feed of the reboiler where the bottoms composition x_b can be measured, and one in the reflux line where x_d can be measured.

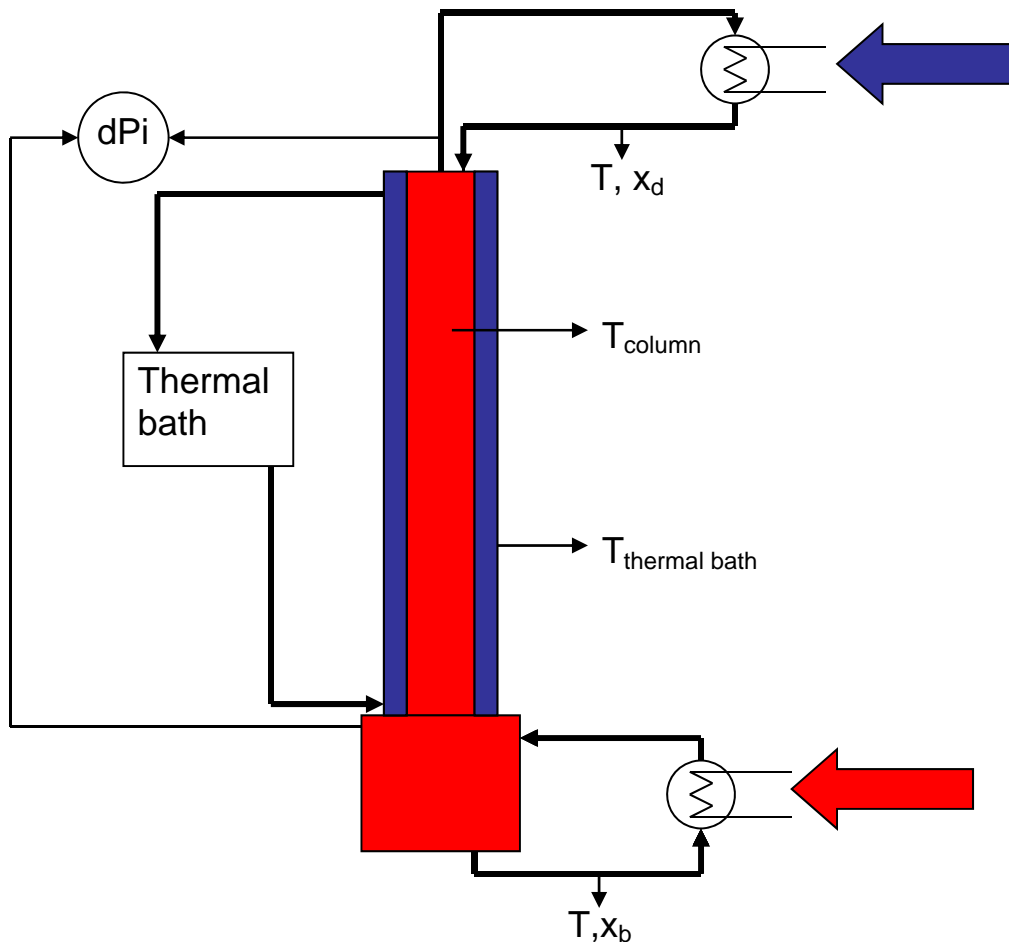


Figure 5 The schematic representation of the PP-HiDiC experimental setup.

1.5 Goals of this research

The Plate-Packing HiDiC has not been tested before at TU Delft or ECN. The goal of this research is to obtain experimental results and evaluate the performance of the PP-HiDiC. Results from predictive models are compared to the experimental results in order to evaluate the models and gain more understanding of the experimental processes. The separation performance (HETP) and the pressure drop are compared to the Delft model. Another goal is to compare the performance of the Plate Packing HiDiC to the Plate Fin HiDiC and data from other packed columns to improve the HiDiC internals.

2. Theory

This chapter describes the theory used to obtain results from the experimental data and the theory behind the Delft model. Not all theory is described, but the most important parameters, like the reboiler stage calculation, F-factor, HETP, main features of the Delft model, Heat transfer and Maldistribution.

2.1 Separation performance: the Fenske equation.

In the experimental setup there are two sampling points. As shown in Figure 5, one is placed in the reflux line, in a bypass around the reflux pump and the other is placed in the reboiler feed line, in a bypass around the reboiler pump.

Using a density meter, the composition of both samples, x_d and x_b , can be found.

With the top and bottom composition and the representative average relative volatility the Fenske equation can be used to determine the number of theoretical (equilibrium) stages for a distillation column operating under total reflux.

$$N_{\text{exp}} = \frac{\ln \left[\frac{x_D}{1-x_D} \cdot \frac{1-x_B}{x_B} \right]}{\ln \alpha_{av}} \quad (2.1)$$

2.2 Reboiler stage calculation

The reboiler of the HIDiC column is a partial reboiler, which means that some separation takes place in the reboiler. In the bottom of the column x_b is measured in the feed line of the reboiler, which means that the separation taking place in the reboiler is part of the separation that is measured.

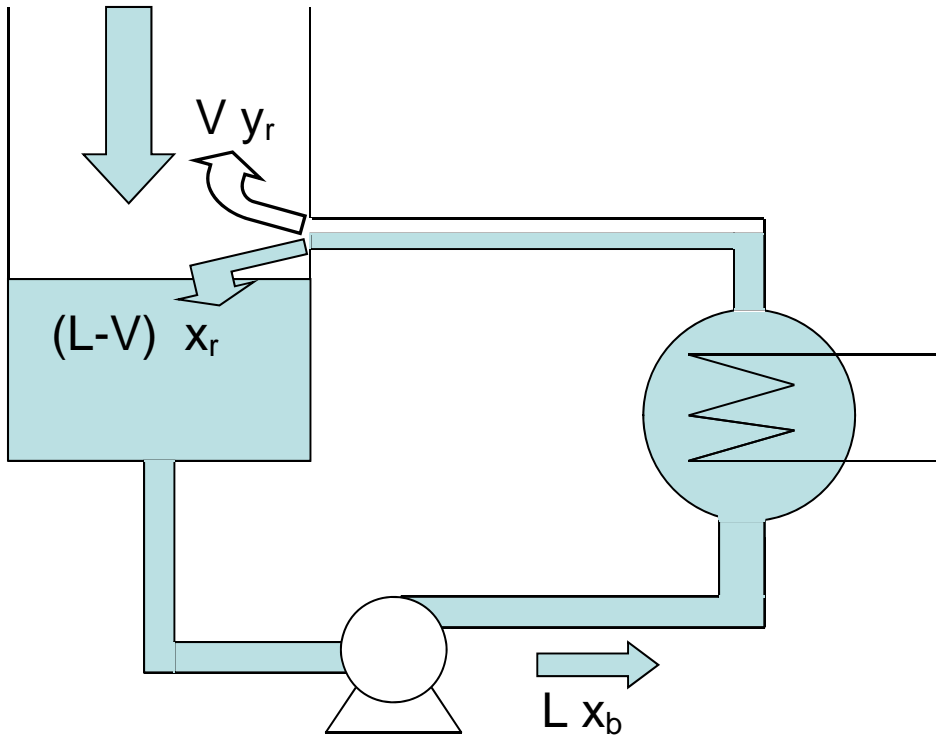


Figure 6 Schematic illustration of the separation in the partial reboiler of the PP-HIDiC experimental setup.

To estimate the separation performance of the column, the amount of separation occurring in the reboiler has to be known. The number of theoretical stages in the reboiler can then be subtracted from the total amount of theoretical stages.

The separation in the reboiler can be estimated using a flash calculation.

First a mass balance over the reboiler (the actual heat exchanger) is made (see Figure 6):

$$y_r = \frac{L \cdot x_b}{V} - x_r \left(\frac{L-V}{V} \right) \quad (2.2)$$

Where L is the flow rate of the liquid stream entering the reboiler and V is the flow rate of the vapour stream leaving the reboiler. Subscript b stands for bottom of the column (the vessel) and subscript r stands for reboiler (the heat exchanger).

The equilibrium equation for a binary system gives:

$$y_r = \frac{\alpha \cdot x_r}{[1 + x_r \cdot (\alpha - 1)]} \quad (2.3)$$

Substitution for y_r gives:

$$\frac{\alpha \cdot x_r}{[1 + x_r \cdot (\alpha - 1)]} = \frac{L \cdot x_b}{V} - x_r \left(\frac{L-V}{V} \right) \quad (2.4)$$

writing x_r explicitly gives 2 solutions:

$$x_r = \frac{a + \sqrt{b - c}}{d} \quad (2.5)$$

(2.6)

With:

$$a = L - V + V \cdot \alpha + L \cdot x_b \quad (2.7)$$

$$\begin{aligned} b = & V^2 \cdot \alpha^2 - 2 \cdot V^2 \cdot \alpha + V^2 - 2 \cdot V \cdot L \cdot \alpha^2 \cdot x_b + 2 \cdot V \cdot L \cdot \alpha \\ & + 2 \cdot V \cdot L \cdot x_b - 2 \cdot V \cdot L + L^2 \cdot \alpha^2 \cdot x_b^2 - 2 \cdot L^2 \cdot \alpha \cdot x_b^2 \\ & + 2 \cdot L^2 \cdot \alpha \cdot x_b + L^2 \cdot x_b^2 - 2 \cdot L^2 \cdot x_b + L^2 \end{aligned} \quad (2.8)$$

$$c = L \cdot \alpha \cdot x_b \quad (2.9)$$

$$d = 2 \cdot V - 2 \cdot L - 2 \cdot V \cdot \alpha + 2 \cdot L \cdot \alpha \quad (2.10)$$

With equation (2.5) y_r can be calculated and the Fenske equation can be filled in. The Fenske equation here is divided into two parts: the separation that takes place in the column, and the separation that takes place in the reboiler.

$$N_{\text{exp}} = \frac{\ln \left[\frac{x_d}{1-x_d} \cdot \frac{1-x_b}{x_b} \right]}{\ln \alpha_{av}} = \frac{\ln \left[\frac{x_d}{1-x_d} \cdot \frac{1-y_r}{y_r} \right]}{\ln \alpha_{av}} + \frac{\ln \left[\frac{y_r}{1-y_r} \cdot \frac{1-x_b}{x_b} \right]}{\ln \alpha_{av}} \quad (2.11)$$

With y_r known, finally with the reboiler stage equation N_{reboiler} can be calculated.

$$N_{\text{reboiler}} = \frac{\ln \left[\frac{y_r}{1-y_r} \cdot \frac{1-x_b}{x_b} \right]}{\ln(\alpha_{av})} \quad (2.12)$$

With the set of equations given above it is possible to estimate the separation in the column and in the reboiler apart from each other.

2.3 HETP

HETP stands for Height Equivalent of a Theoretical Plate. With the adapted Fenske equation the amount of stages in the column is calculated. The HETP can be calculated by dividing the height of the packed bed by the amount of theoretical stages, as shown in equation(2.13).

$$HETP = \frac{h_{\text{packedbed}}}{N_{\text{Fenske}}} \quad (2.13)$$

The HETP is a measure for the efficiency of a distillation column. The height of the packed bed is not the same as the height of the distillation column, because in a packed column redistributors are needed, which are not included in the bed height.

2.4 F-factor

The superficial velocity of a gas alone is not a good measure for the vapour load in a distillation column, because the density of a gas is strongly dependent on the temperature, pressure and composition of the gas. To be able to compare the gas load in distillation columns, the F-factor ($\text{Pa}^{0.5}$) is introduced. The F-factor is the product of the superficial velocity and the square root of the density of the gas.

$$F = u_g \sqrt{\rho_g} \quad (2.14)$$

The F-factor can be compared to the kinetic energy of a gas. Even if different operating pressures or components are used, if the F-factor in two situations is the same, the situations are comparable.

In the case of a total reflux column, the F-factor and the reflux stream are coupled because all vapour is condensed and returned as the liquid to the column.

2.5 Flooding

In a tray column, if the gas load is too low, liquid can leave the tray via the holes in the plate. This weeping is unwanted because liquid from different trays can mix, which reduces the separation. When the gas load is too high, entrainment occurs when the gas takes liquid with it to the next stage. This is like weeping unwanted and creates borders for stable operation. The F-factor has thus a lower and an upper limit between which stable operation is possible. In a packed column there is no such thing as weeping, i.e. a lower operating limit. The liquid always flows over the packing surface, but at low liquid loads and F-factors may happen, mainly because of malfunctioning of a distributor that not all surface in the column is wetted. The region at low F-factors is called the preloading region. As shown in Figure 7, until the loading region is reached, the capacity of the column increases while the HETP does not increase a lot because extra surface in the column is wetted.

In the loading region the HETP decreases due to increased friction between gas and liquid, which leads to intensified mass transfer¹².

When the F-factor increases more, the thickness of the liquid film over the packing surface are increases, making mass transfer less efficient. Also the effective packing surface decreases. The HETP increases rapidly due to these effects, which means the separation process is less efficient.

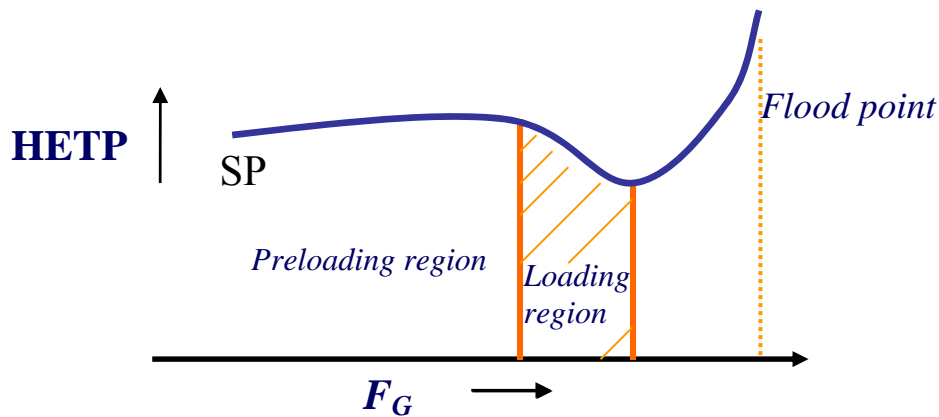


Figure 7 A typical efficiency curve for structured packing¹²

2.6 Delft model

The Delft model can predict mass transfer and pressure drop of a packed column based on the geometry of the structured packing. Basic geometry dimensions required by the Delft model are shown in Figure 8. Because this model allows the user to adjust the model to the geometry of the column, it seems to be suitable for simulating the PP-HiDiC. Input variables for the Delft model are the corrugation inclination angle α with respect to horizontal, crimp angle β , the porosity of the packing ε , the corrugation height h_{cor} , the corrugation base b , which is the perpendicular distance between two corrugations, the length of a corrugation side s , the height of a packing element h_{pe} , the number of packing elements n_{pe} . The gas and liquid diffusion coefficients D_G and D_L , the density of the gas and liquid ρ_g , ρ_l , the viscosity of the liquid and gas μ_g and μ_l , the surface tension σ , and the stripping factor λ . A complete description and all equations and expressions can be found elsewhere¹³.

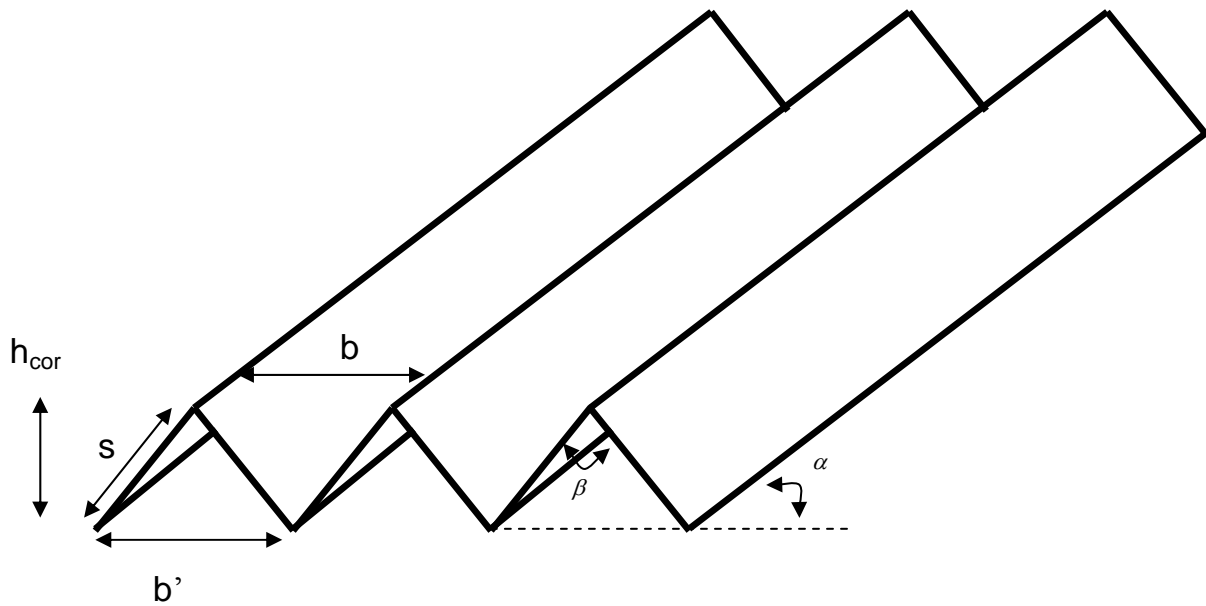


Figure 8 A corrugated sheet with the main dimensions.

2.6.1 Pressure drop in the Delft model

For modelling pressure drop the Delft model makes distinction between preloading and loading regions.

The preloading pressure drop composes of three components that cause friction:

$$\Delta p_{GL}$$

The gas flowing up through the column contacts the liquid which is flowing down along the packing. This contact causes a resistance or pressure drop.

$$\Delta p_{GG}$$

In the packing material there are mixing points at which gas from different channels mixes. This mixing results also in pressure drop.

$$\Delta p_{DC}$$

The packing contains numerous sharp edges. At these sharp edges, the gas has to change direction which causes a pressure drop.

At a certain point there must be a transition from the preloading range to the loading range. This point is called the loading point. In the Delft model, the loading point is calculated and from the loading point on, the preloading pressure drop is corrected with a loading factor.

2.6.2 Mass transfer in the Delft model

In the Delft model the HETP is used to express mass transfer. The HETP is in this case calculated by

$$HETP = \left[\frac{\ln \lambda}{\lambda - 1} \right] \cdot [HTU_G + \lambda \cdot HTU_L] \quad (2.15)$$

Here λ is the stripping factor and HTU stands for Height of a Transfer Unit for both the gas and liquid phase.

HTU_G and HTU_L are calculated by

$$HTU_L = \frac{u_{Ls}}{k_L \cdot a_e} \quad (2.16)$$

$$HTU_G = \frac{u_{Gs}}{k_G \cdot a_e} \quad (2.17)$$

As stated above, a detailed description of the model can be found elsewhere.¹³

2.7 Heat transfer

In the HIDiC column heat is transferred between the thermal bath fluid side and the column. The heat transferred from the hotter to the cooler side is described by.¹⁴

$$Q = U \cdot A \cdot \Delta T \quad (2.18)$$

Where U is the overall heat transfer coefficient, defined as:

$$\frac{1}{U} = \frac{1}{h_{column}} + \frac{d}{\lambda_{wall}} + \frac{1}{h_{thermalbath}} \quad (2.19)$$

Here h_{column} is the heat transfer coefficient on the distillation side, $h_{thermalbath}$ is the heat transfer coefficient on the thermal bath side and λ_{wall}/d is the heat transfer coefficient through the wall of the column. In the PP-HIDiC, the wall of the column is kept as thin as possible, and in the thermal bath side of the column fins are placed. This means the resistance to heat transfer is located at the column side. This term is the dominating term of the three shown in equation(2.19).

2.8 Maldistribution

In all packed distillation columns to some extent maldistribution occurs. Maldistribution is uneven distribution of liquid and/or vapour across the cross sectional area of the column. It is mainly caused by a poorly functioning liquid distributor or it can develop within the packing itself due to irregularities in the structure of the packed bed or because of wall flow.¹⁵ Maldistribution causes a packed column to work less efficiently. If maldistribution is severe, it is possible that not all surface area in the column is wetted. This means the effective surface area in the column decreases which means there is less contact between liquid and vapour, resulting in a worse separation.

Billingham and Lockett¹⁵ stated that in a column with a fixed number of stages, the sensitivity to maldistribution increases as the relative volatility increases.

So experiments can be carried out with different concentrations of the high volatility component, to check for indications of maldistribution. In this way one can see if there is severe maldistribution in the distillation column.

3. Experimental

This chapter describes the experimental setup, data processing and the adaptations made to the Delft model. All concentrations are written as the fraction cyclohexane.

3.1 Experimental setup

The experimental setup is one half of a HIDiC. It can be operated as a stripping section or as a rectifying section of a HIDiC. To isolate the effect of heat transfer on pressure drop and separation, the column can also be operated adiabatically.

As shown in Figure 9, the reboiler section consists of a pump (P-101), a vessel under the column (V-103) and a heat exchanger (E-101) where the liquid is heated using steam. The heated vapour liquid mixture enters the bottom section, i.e. the vessel which is placed directly under the PP-HIDiC. The vapour then enters the HIDiC and is partly rectified against the down coming liquid from the condenser. The vessel V-101 is a safety vessel, i.e. in case of emergency the liquid from the column can be emptied into vessel V-101.

The column itself, PPHE, is tested in two different setups: a plate fin and a plate packing column which both are 1000 mm x 200 mm x 15 mm. The walls of 1000 mm x 200 mm are double walled and fluid from a thermostatic bath (E103) is flowing in this space. This way the column can be heated or cooled to simulate a stripping or a rectifying section of a HIDiC respectively. In adiabatic operation the thermostatic bath is turned off and the oil is stagnant and acts as insulation.

On top of the column a liquid distributor is placed. Here the reflux stream is distributed equally over the whole cross section of the column. Vapour can pass the distributor and is condensed in the condenser (E102).

The liquid from the condenser is collected in a vessel (V-102) and pumped back into the column. The vessel is a buffer to create a constant reflux stream through the column. The reflux is pumped back into the column from the vessel (V-102) by a pump (P-102).

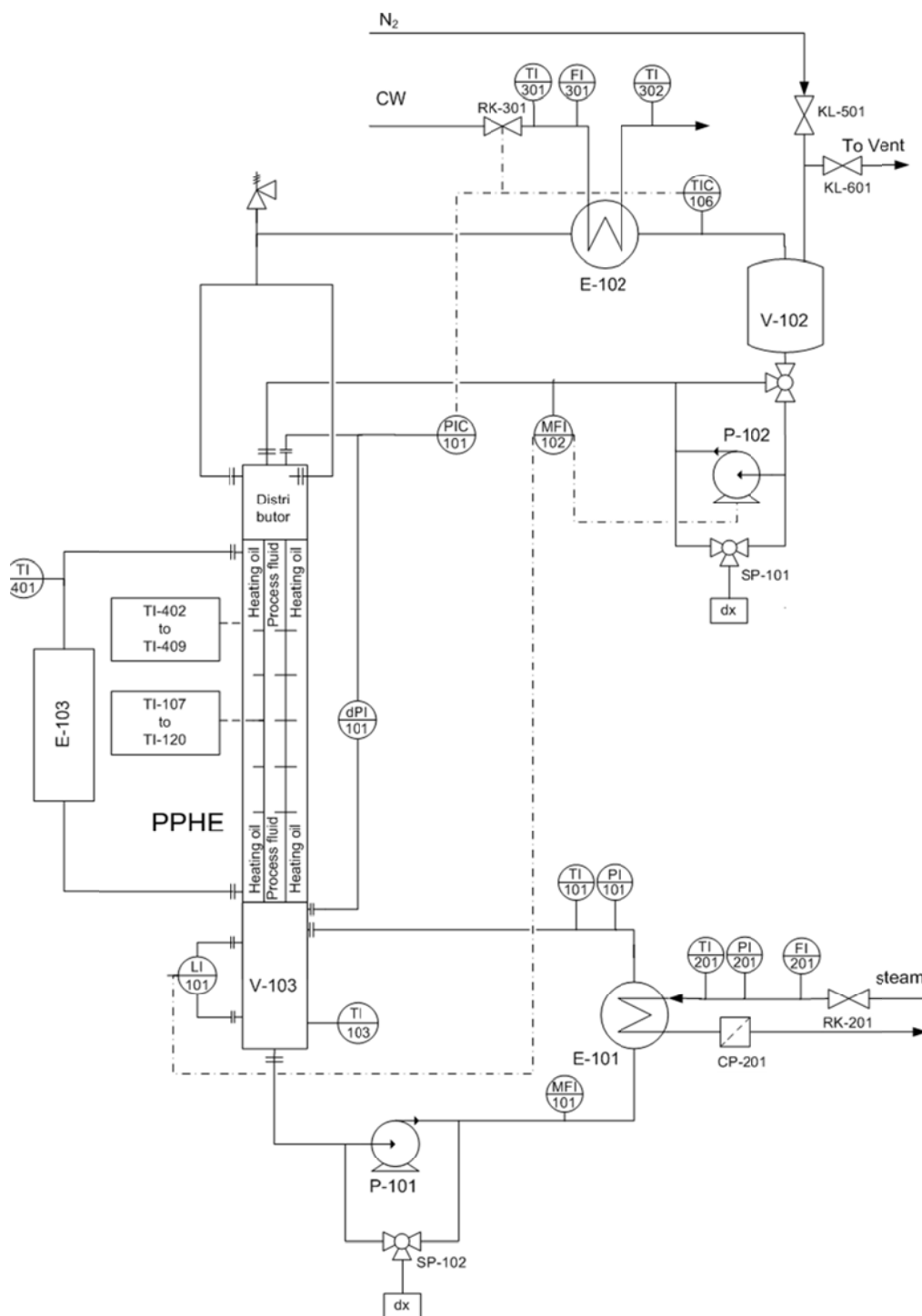


Figure 9 Flow sheet of the experimental setup.

3.2 Column internals

The PP HiDiC internals, made by ECN, are two plates of 1000x200 mm with each 5 200x200x7 mm plates of Mellapak 350Y (see Figure 8) mounted on it in zigzag configuration. The two plates are mounted together with the two layers mirrored towards each other and a perforated plate in between. This plate effectively increases installed specific geometric area but prevents interaction of vapour and liquid streams from neighbouring flow channels. As shown in Figure 11 the PP-column consists of two parallel units with fully closed flow channels, resembling a monolith like structure but with inclined channels.

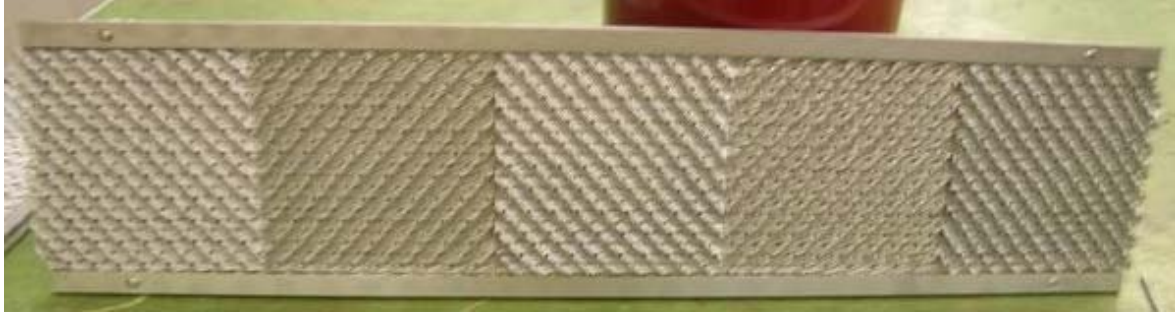


Figure 10 side view of one of the sides of the column.

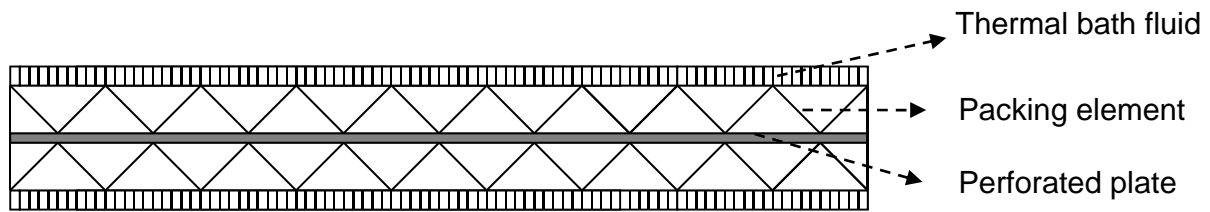


Figure 11 Top view of the PP-HiDiC column.

3.3 Pressure drop

The pressure drop in the column is measured using a GE Druck STI 2100 dPi sensor which is connected between the top of the column and a bypass which comes from the bottom of the column. A pressure difference of 0-10 mbar can be measured.

3.4 Internal reflux

As stated by M. Strijker¹⁶ the external reflux in the HiDiC setup is sub cooled. This means the internal reflux is larger than the external reflux due to condensation of vapour. To calculate the internal reflux equation (3.1) is used¹.

$$R_{\text{internal}} = R_{\text{external}} \left(\frac{1 + C_p \Delta T_{\text{subcooling}}}{\Delta H_{\text{vap}}} \right) \quad (3.1)$$

Where C_p is the specific heat, ΔH_{vap} is the heat of vaporization and:

$$\Delta T_{\text{subcooling}} = T_{\text{column}} - T_{\text{reflux}} \quad (3.2)$$

3.5 Delta T calculations

The average temperature of the column is calculated by using the readings of sensors TI-402-TI-404 and TI-406-TI-409. These sensors are placed in the thermostat liquid side of the column. Sensor TI-405 has a bias and is therefore not taken into account. The sensors in the process side of the column have a large spreading in the readings and therefore there was chosen to use the sensors of the thermostat liquid side.

The temperature difference between a diabatic and an adiabatic measurement is calculated by subtracting the average temperature of the thermostat liquid inside the column in the adiabatic

measurement from the average temperature of the diabatic measurement. Due to the insulation, the temperature of the thermostat liquid for the adiabatic situation is considered to correspond well to the temperature of the process fluid at the given height in the column.

3.6 F-factor calculation

To calculate the F-factor in the column, first the superficial gas velocity is needed:

$$u_g = \frac{M_G}{\rho_g \cdot A} \quad (3.3)$$

Because the column is operated at total reflux, the liquid and gas mass streams in the column, M_L and M_G are equal and M_L can be substituted for M_G in equation (3.3). This is done because M_G is not measured in the experimental setup.

With the superficial gas velocity known, the F-factor in the column can be calculated by

$$F = u_g \cdot \rho_g \quad (3.4)$$

In diabatic measurements the F-factor is not constant over the column because vapour is condensed or liquid is evaporated in the rectifying and stripping mode respectively. Therefore also the bottom F-factor is calculated. In fact, the bottom F-factor is the F-factor from the adiabatic measurement with the same reboiler duty as the diabatic measurement, calculated as outlined above.

The average F-factor is the average value of the top and bottom F-factors.

3.7 Delft model

The Delft model is designed for the modelling of cylindrical packed columns. It is however possible to model a different column with the Delft model, because the input variables are for a large part packing specific geometrical variables. Therefore, the PP-HIDiC was modelled with the Delft model by making some adaptations.

The diameter of the column is 0.2 m. In the model, this would mean that there is a cylindrical column with a diameter of 0.2m but instead of a cylinder with a diameter of 0.2 m, only a slice around the diameter of the column is used to model the PP-HIDiC as is shown in Figure 12.

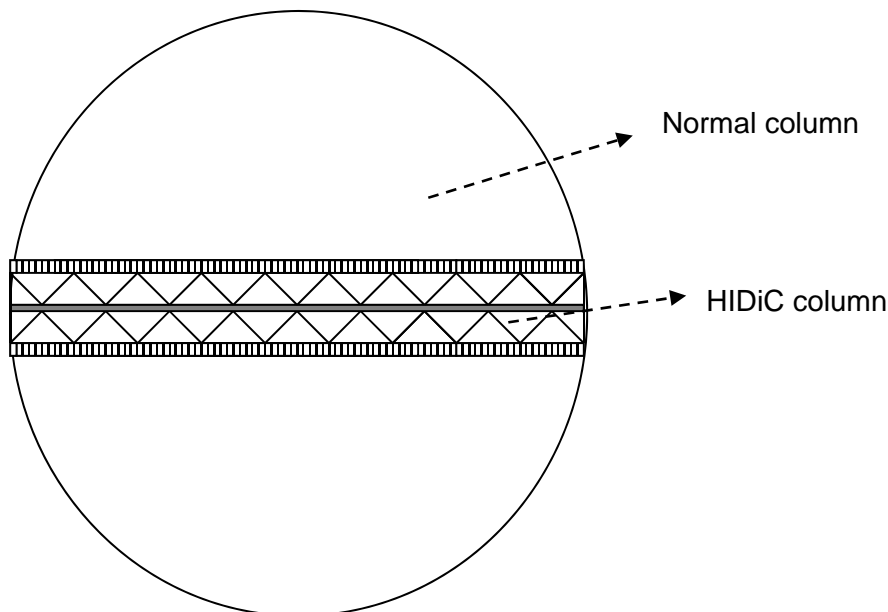


Figure 12 PP-HiDiC top view indicating the relative size of the rectangular cross sectional area with respect to that of a cylindrical column with a diameter of 20 cm.

The perforated plate in between the two packing elements creates extra surface area in the column. The total surface area of the column exists of the area of the packing, the walls and the plate. The specific surface area is calculated by taking the sum of these three elements.

The Delft model simulates the packed column with triangular channels. As shown in Figure 13, two of the three sides of these channels are liquid covered packing sheet and the third side of the channel is a gas/gas interface where gas from the one channel interacts with gas from another channel. In the model this means there are two gas/liquid interfaces and one gas/gas interface.

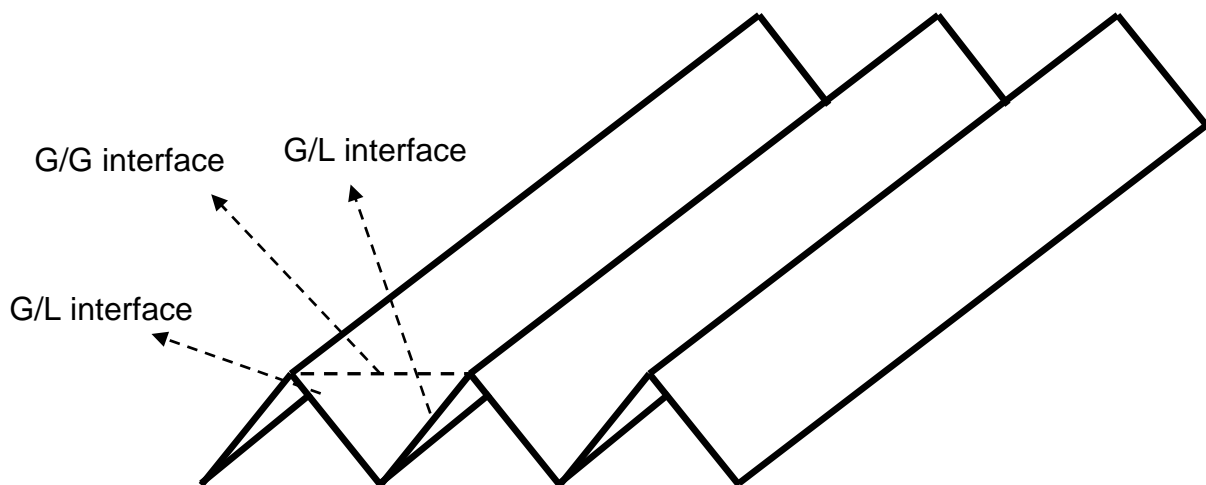


Figure 13 Interfaces on a corrugated sheet packing element.

If a perforated plate is installed in between two corrugated sheets, the triangular channels in the column are closed as shown in Figure 14. So instead of two now all three sides of the triangular channel are gas/liquid interface. To correct for this, ϕ (the part of the surface of the triangular channel on which a gas/liquid interface is present) is set to 1. This cancels out the gas/gas interaction term in the pressure drop calculations.

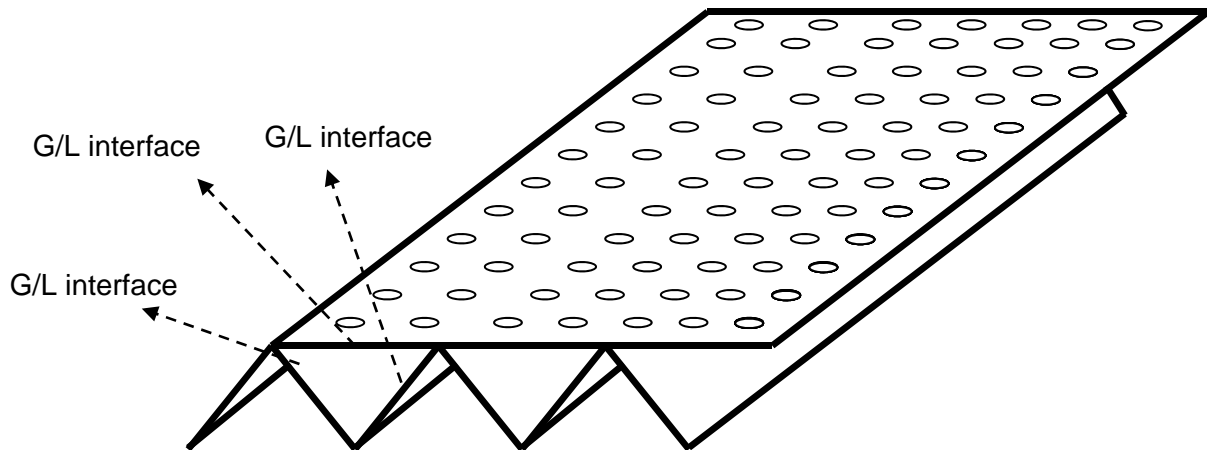


Figure 14 Interfaces on a corrugated sheet packing element with a perforated plate placed on top of it.

In the Delft model the Onda correlation is used to predict the effective area of the packing. In this study the Onda correlations are not used, instead the total specific surface area is used as effective area. This shows the maximum separation the column should be able to reach, provided all three sides of the channels are fully covered by a uniform liquid film. Also, the model can be used to determine the effective area complying with the experimentally determined separation efficiency, which is a good indication of the fraction of installed area used.

The loading point (F_{load}) has been shifted in the model towards a higher F-factor to fit the pressure drop data better in the loading region. This is done by multiplying the equation for F_{load} with a factor until it fitted well.

3.8 Heat transfer

To calculate the heat transfer in the diabatic measurements, the difference in internal reflux is used to calculate Q_{HIDiC} . For all series of measurements used, one adiabatic and at least one diabatic measurement are carried out with the same reboiler duty.

$$Q = (F_{diabatic} - F_{adiabatic}) \cdot \Delta H_{vap} \quad (3.5)$$

In a diabatic measurement the size of the reflux stream is different from an adiabatic measurement because in a diabatic measurement the column is heated or cooled by the thermostatic bath, which causes extra evaporation or condensation in the column respectively. The column is operated at total reflux, so difference in reflux flow between the diabatic and the adiabatic measurement is a measure for the heat transferred to or from the thermostatic bath.

This method is more reliable than using the condenser duty, because the reflux stream is cooled down to a temperature lower than the boiling point and because the cooling water flow cannot be measured very precise.

With the HIDiC duty Q_{HIDiC} known, it is possible to calculate the value of UA, i.e. the heat transfer coefficient times the surface area with

$$UA = \frac{Q_{HIDiC}}{\Delta T} \quad (3.6)$$

The overall heat transfer coefficient U can be calculated by dividing by the heat transfer surface of the column A. For the surface, different values can be used. In this case, the area of the wall itself is used. The area of the fins in the cooling/heating compartment and the packing surface are not used.

3.9 Relative volatility

The relative volatility is used in for example the Fenske equation. The relative volatility can be calculated with different models, for example the van Laar equation, the Margules equation, Wilson, NRTL, or some other thermodynamic model.

To find a suitable model for the relative volatility, different models have been tested by calculating the composition of a vapour in equilibrium with a liquid using equation (3.7).

$$y = \frac{\alpha \cdot x}{1 + x \cdot (\alpha - 1)} \quad (3.7)$$

The Vapour Liquid Equilibrium Data Collection¹⁷ contains experimental data on the cyclohexane/n-heptane mixture. For each set of experimental data from the Vapour Liquid Equilibrium Data Collection a model is pointed out which fits best. Three of those models and the relative volatility calculated in Aspen Dynamics using the NRTL model are compared to experimental data (in the composition range used in the experiments) from three different experimental data sets from the Vapour Liquid Equilibrium Data Collection. The model with the least deviation from the experimental data is used.

The model with the smallest deviation from the data points from the different experimental data series was the Margules equation. The Margules equation is used to calculate the activity coefficient with values for the constants A_{12} and A_{21} as shown below.

The Margules equations with the constants A_{12} and A_{21} fits experimental data¹⁸ which can be found on page 304 in the Vapour Liquid data collection¹⁷.

$$\log \gamma_1 = x_2^2 [A_{12} + 2 \cdot x_1 (A_{21} - A_{12})] \quad (3.8)$$

$$\log \gamma_2 = x_1^2 [A_{21} + 2 \cdot x_2 (A_{12} - A_{21})] \quad (3.9)$$

To calculate the relative volatility, also the partial pressure P_i^{sat} is needed. This is calculated using equation (3.10)

$$\log P_i^{sat} = A - \frac{B}{C + T} \quad (3.10)$$

With the partial pressure and the activity coefficient the relative volatility can be calculated by equation (3.11).

$$\alpha = \frac{P_{ch}^{sat} \cdot \gamma_{ch}}{P_{Nh}^{sat} \cdot \gamma_{Nh}} \quad (3.11)$$

The constants used from the Vapour Liquid Equilibrium Data Collection are:

$$A_{ch}=6.85146$$

$$B_{ch}=1206.47$$

$$C_{ch}=223.136$$

$$A_{nh}=6.89386$$

$$B_{nh}=1264.37$$

$$C_{nh}=216.64$$

$$A_{12}=0.0563$$

$$A_{21}=-0.0938$$

3.10 Properties of the mixture

The test fluid used in the experiments is a mixture of cyclohexane and n-heptane. Of both liquids the pure component properties can be found using Fluidprop.¹⁹ The properties of the mixture are however not available from Fluidprop.

The density of the liquid is calculated using equation (3.12).²⁰

$$\rho_{l,mix} = x_{ch} \cdot \rho_{ch} + (1 - x_{ch}) \cdot \rho_{l,nh} \quad (3.12)$$

The density of the vapour is calculated in a similar way, using the density of both components in the vapour phase instead.

The viscosity of the liquid is calculated with equation (3.13)²⁰

$$\mu_{l,mix} = \left[x_{ch} \cdot \mu_{l,ch}^{1/3} + (1 - x_{ch}) \cdot \mu_{l,nh}^{1/3} \right]^3 \quad (3.13)$$

3.11 Analysing the samples

The samples taken from the column were analysed in the lab using a density meter. The Anton Paar DMA 5000 density meter gives the density at 20°C in 6 decimals. Using the relation between the density and the composition of the mixture, the composition of the mixture can be found.

4. Results and discussion

In this chapter experimental results and results from the Delft model are discussed.

4.1 Mass transfer

The adiabatic mass transfer performance of the HiDiC is shown in Figure 15 together with results from the Delft model.

Figure 15 shows a decreasing HETP at higher F-factors, which means mass transfer is more efficient at a higher F-factor. Measurements above an F-factor of $2.6 \text{ Pa}^{0.5}$ were not possible because of the limiting capacity of the reflux pump P-102.

A decreasing trend in HETP is also shown in Figure 7 in the loading regime of a packed column. From a comparison with Figure 7 can be concluded that the optimum F-factor can be higher than $2.6 \text{ Pa}^{0.5}$, at a certain moment HETP has to rise again due to flooding which is not found in the measurements.

In comparison with the B1-400 and B1-250 packing from J. Montz the flooding point in the HiDiC column is located at a higher F-factor. In the B1-400 and B1-250 packing the flooding points are located at an F-factor of $2.3 \text{ Pa}^{0.5}$ and $2.5 \text{ Pa}^{0.5}$ respectively^{21,22}. This means the HiDiC column can handle a higher gas load before enhanced liquid holdup or back mixing makes the separation worse. A reason for this can be the absence of gas/gas interaction and therefore less turbulence in the gas phase. The liquid and gas therefore can flow smoother along each other.

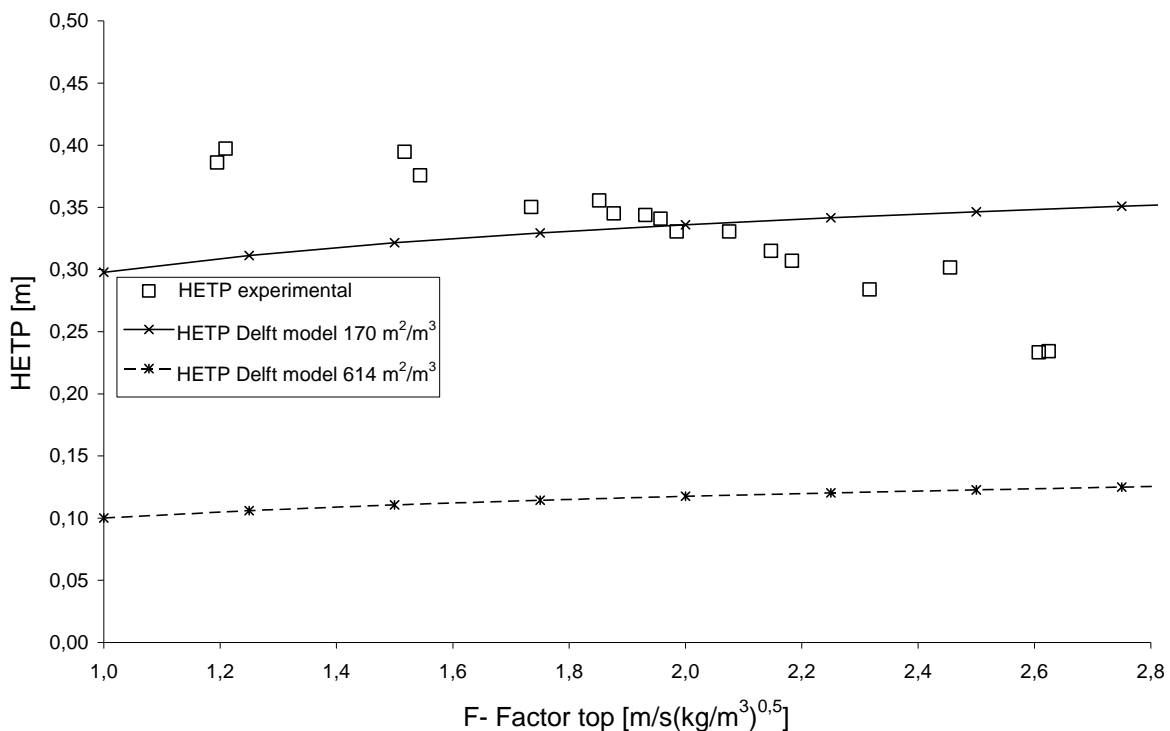


Figure 15 measured vs. predicted mass transfer as a function of F-factor.

The Delft model, assuming that the installed area is fully utilized, predicts a much lower HETP than is found in the measurements. For a specific area of $170 \text{ m}^2/\text{m}^3$ the average HETP is equal to the average HETP found in the experiments. This is much less than the $614 \text{ m}^2/\text{m}^3$ installed in the column.

Olujčić et al²³ and Behrens et al²⁴ found similar results in simulations of modified packing with a metal sheet placed between the layers to create extra surface area.

The Delft model shows the trend that is expected from a structured packing distillation column. This trend differs from the experimental data. For the Delft model, HETP increases with increasing F-factor, while for the experimental data the HETP decreases at a higher F-factor.

This decrease in HETP means the PP-HiDiC operates more efficient at higher F-factors.

In the Delft model, the HETP is calculated via the HTU. This HTU is calculated, as shown in equation (2.16) by dividing the superficial liquid velocity by the liquid mass transfer coefficient times the effective area.

In the simulations done with the Delft model, the effective area was kept constant, but the decreasing HETP in the experimental data shows the effective area in the column probably increases with increasing F-factor. At a higher F-factor, the gas and liquid streams through the column are larger. These larger streams can cause a better distribution of liquid along the column cross sectional area and therefore cause a larger effective area.

The difference in performance between the Delft model and the experimental data can be explained by different factors.

The perforated plate closes off the packing, which results in triangular channels through which vapour and liquid flows without any interaction. Liquid and vapour from different channels cannot mix well and it is possible that the liquid is not evenly distributed over the channels in the packing. The plate also creates corners in the triangular channels in which the liquid can collect. The liquid is then not well distributed over the channel surface, but the major part flows as a rivulet in the lowest corner of the packing channel. Because the PP-HiDiC is operated at total reflux, at higher gas loads also the reflux increases. This extra liquid and vapour may cause a better distribution of the liquid over the column cross sectional area, enlarging the effective area in the column. Also, the liquid in the triangular channels is forced out of the corners at higher gas loads, which causes the column to operate more efficiently.

The decrease in performance predicted by Olujčić et al²³ was however less dramatic than the performance drop found in the experiments. It is possible that due to maldistribution not all channels in the packing material are used. This is discussed later on.

In comparison with the PF-HiDiC, mass transfer in the PP-HiDiC is much more efficient, as the average HETP in experiments done with the PF-HiDiC was 144cm and the average HETP for the PP-HiDiC is 33 cm, which means mass transfer in the PP-HiDiC is thus at least 4 times as efficient as in the PF-HiDiC. The main reasons for this can be the longer residence time of the liquid and a larger part of effective area in the PP-HiDiC, as in the PF-HiDiC there are no bends, only straight channels, which means liquid can fall down fast, a part of it possibly without touching the column walls.

4.2 Pressure drop

The pressure drop over the HiDiC shows a trend as expected from a packed column^{21,22}. As shown in Figure 16, the pressure drop increases slowly in the preloading regime and beyond the loading point it increases faster. The experimental pressure drop shows a clear loading and preloading region, with the loading point located at $1.9\text{Pa}^{0.5}$. The Delft model predicts after shifting the loading point from $1.7\text{Pa}^{0.5}$ to $1.84\text{Pa}^{0.5}$ a similar pressure drop as measured. In the preloading regime pressure drop is higher than modelled, which can be caused by the

large amount of channels in the packing elements that end at the wall of the column, as shown in Figure 10 .

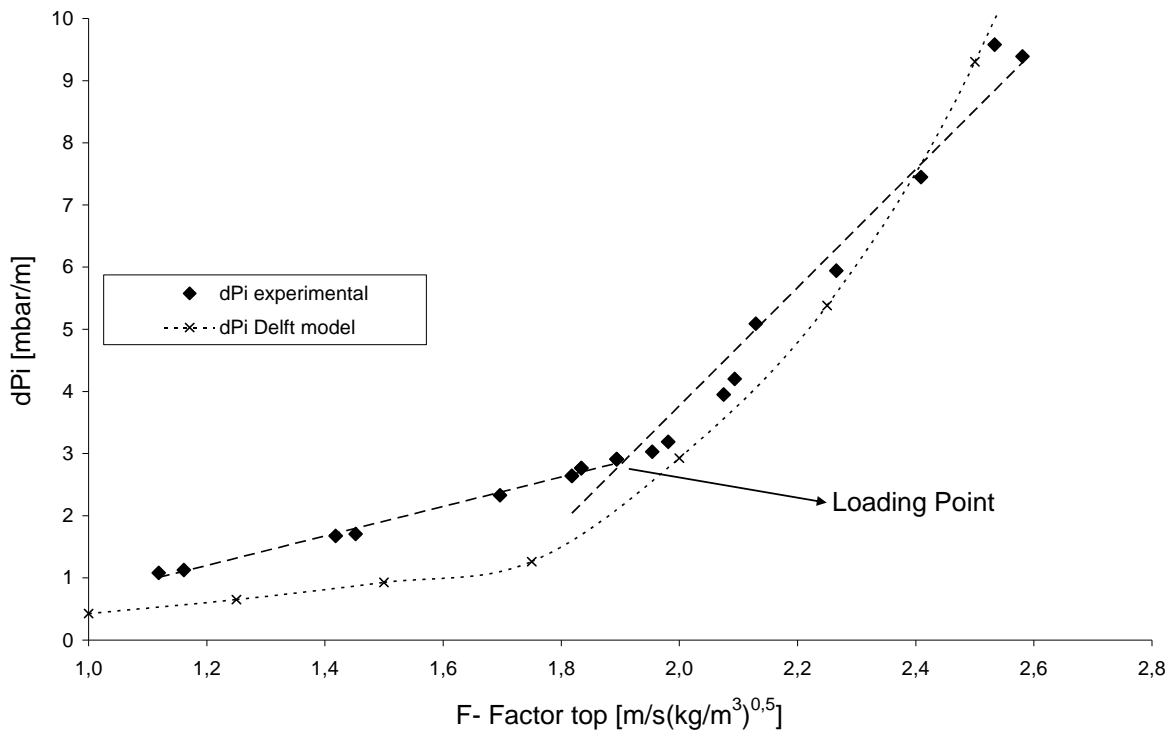


Figure 16 Measured vs. Predicted pressure drop as a function of F-factor

At the column wall the vapour, prevented by the wall wipers to flow upwardly along the wall, is forced to make a sharp turn and enter the flow channels oriented upwardly. This wall effect is in the HiDiC column much larger than in a conventional column and can be the cause for the higher pressure drop in the preloading regime.

In Figure 16, the pressure drop is plotted against the F-factor in the top of the column. In the diabatic measurements, the F-factor is not constant over the column. In rectifying mode, there is condensation in the column, so the bottom F-factor is higher than the top F-factor. For a similar top F-factor, the average F-factor in the column is higher in rectification mode, and lower in stripping mode. Therefore, in Figure 17 the average F-factor over the column is used. The pressure drop data as a function of the average F-factor from the diabatic measurements show the same trend as the adiabatic measurements. There seems to be no effect of heat transfer on pressure drop.

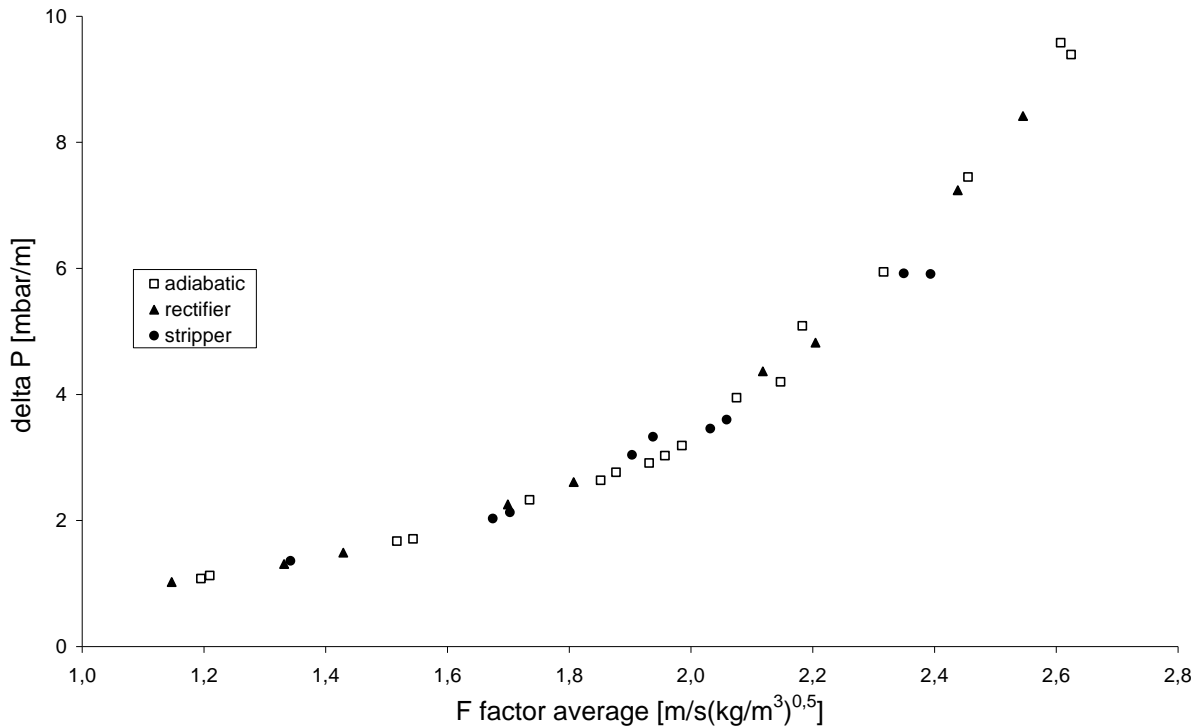


Figure 17 The effect of operating mode on the pressure drop.

4.3 Reboiler stage calculation

The separation in the reboiler and in the column was calculated separately by the adapted Fenske equation, as done in all measurements. Because in the three measurements shown in Figure 18 the reboiler duty was kept constant, the separation in de HIDiC column should be the same. The circulation rate through the reboiler was changed however, and it should cause a difference in separation in the reboiler.

Figure 18 shows that the major part of the difference in the total amount of stages is indeed caused by the changed reboiler circulation in this set of experiments. The F-factor in the column was not completely constant, which can be an explanation for the small deviation in the amount of stages in the HIDiC. The deviation however is quite small so from these experiments it can be concluded that the method used to calculate the separation in the column apart from the reboiler is quite accurate. Therefore, these calculations have been used to calculate the separation in all experiments described in this report.

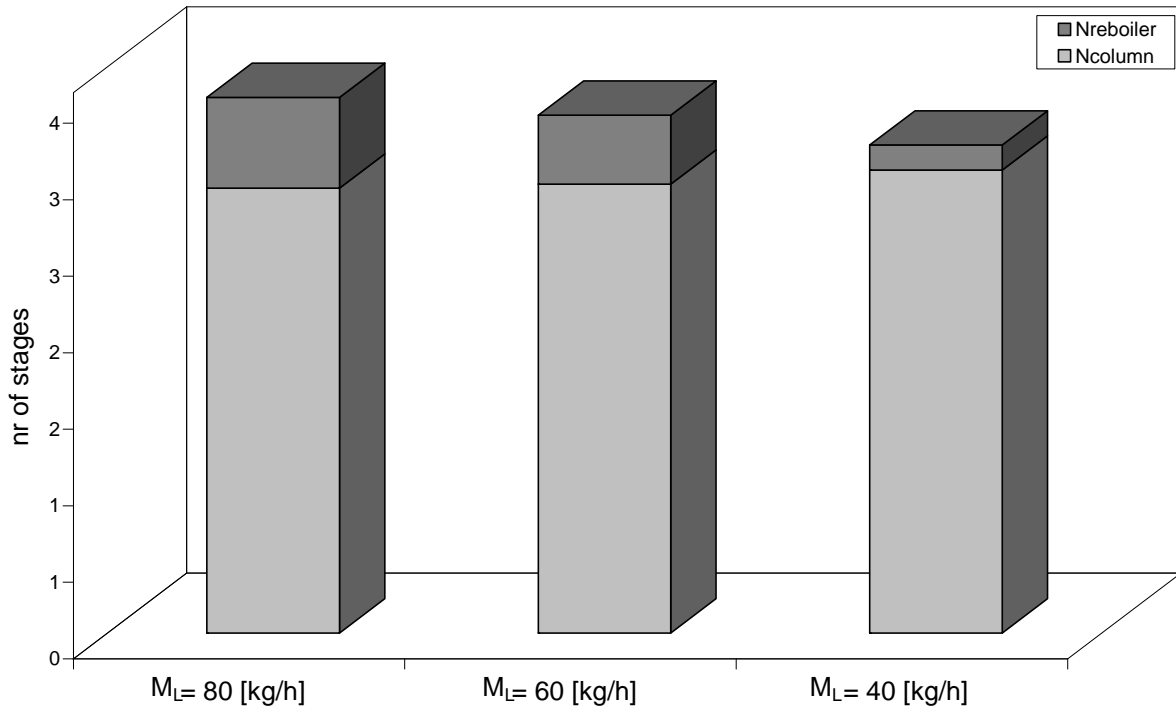


Figure 18 Distribution of stage requirement as a function of the liquid load of the reboiler

4.4 Heat transfer

In Figure 19 the heat transfer between the distillation section and the cooling/heating section of the HIDiC is plotted against the temperature difference. The slope of the trend line plotted gives UA . This trend line should go through zero, because when there is no temperature difference, no heat can be transferred. When a trend line is plotted it will not go through zero, but forcing it through zero gives only a small deviation. In this case the slope becomes 337 W/K instead of 335 W/K.

The column walls have a total area of 0.4 m^2 . This gives an overall heat transfer coefficient U of $844 \text{ W/m}^2\text{K}$ in the column.

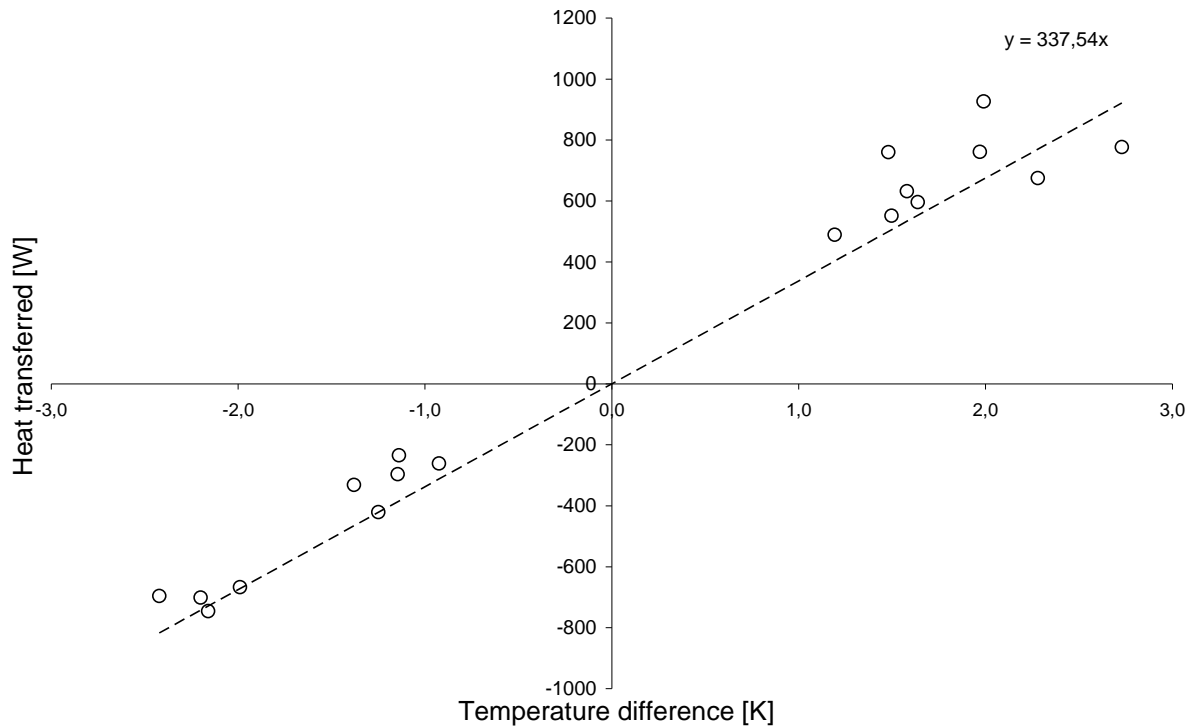


Figure 19 Heat duty of the PP-HIDiC as a function of temperature difference

As shown in Figure 20 the effect of heat transfer on mass transfer is small. In all three modes of operation the same trend can be seen, HETP tends to decrease with increasing F-factor. A more detailed elaboration of heat transfer effects is shown in Figure 21, where HETP is shown as a function of heat transfer duty of the HIDiC with the F-factor as a parameter. For each series of measurements the F-factor at the bottom is equal, while different amounts of heat are transferred. The HETP seems to be the highest in the stripping mode and tends to decrease when the column is operated adiabatically. In rectifying mode the HETP tends to be even lower as in adiabatic operation.

The average value between the stripping and rectification mode is however similar to the HETP found in adiabatic operation. Therefore it may be concluded that there is no net effect of heat transfer on mass transfer in the HIDiC column. In the design of a HIDiC column, it can be wise to take into account that HETP in the stripping section is higher than in the rectification section.

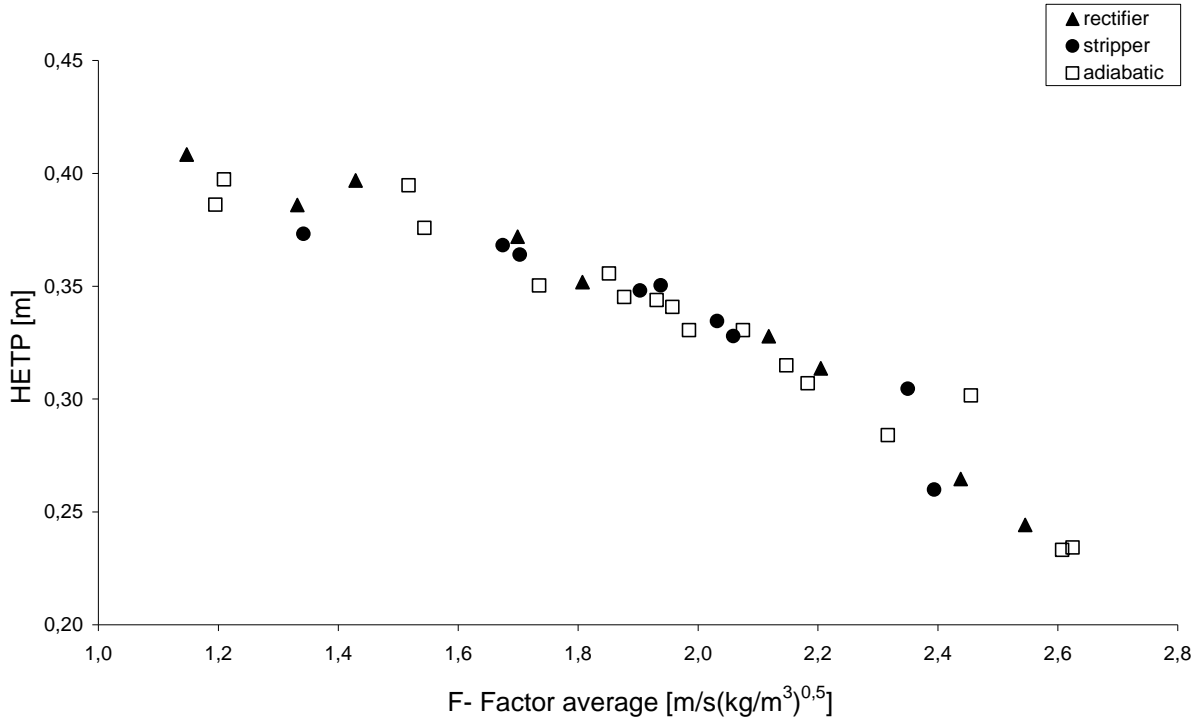


Figure 20 Effect of the operating mode on the efficiency of the PP-HiDiC

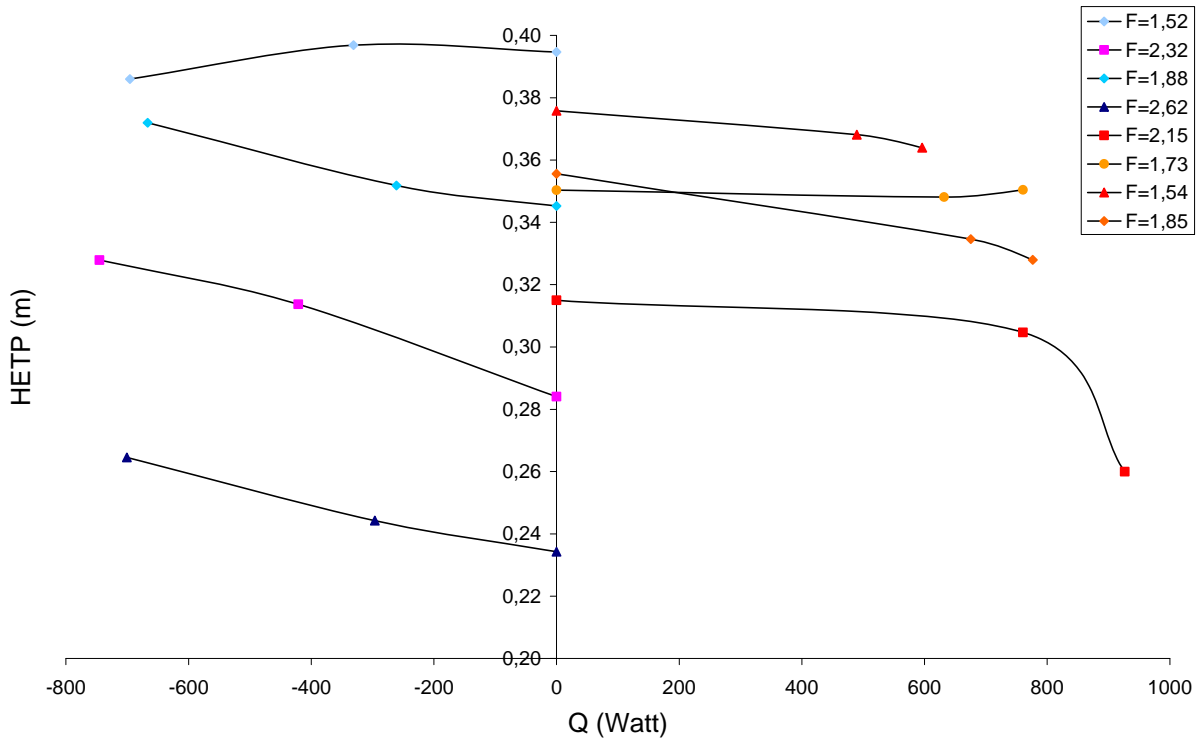


Figure 21 HETP as a function of HiDiC duty with the F-factor as a parameter.

4.5 Maldistribution

Maldistribution adversely affects the efficiency of a packed distillation column. It is therefore important to know if maldistribution was an issue in the HIDiC experimental setup. In a future HIDiC project this can be taken into account in the design of the column.

Figure 22 shows what is expected from calculations. If the relative volatility is higher, separation is easier and the HETP will be lower.

For the cyclohexane/n-heptane mixture used, the relative volatility as calculated with the Margules equations changes not much with concentration. A lower concentration of cyclohexane gives a higher relative volatility.

For the measurements at $x_b=0.35$ the relative volatility is the highest and the HETP exhibits the lowest values. For $x_b=0.85$ the relative volatility is slightly lower than in experiments at $x_b=0.7$. The HETP in both experiments are similar, although in experiments with $x_b=0.85$ HETP is slightly higher, which is in agreement with what is expected from the slightly lower relative volatility. This composition effect is normal behaviour of a distillation column.

A higher relative volatility makes a packed column more sensitive for maldistribution as stated by Billingham¹⁵. Maldistribution results in a lower separation efficiency, and therefore a higher HETP. The method of Billingham however, is made for large scale columns where maldistribution is less severe as is expected in the experimental PP-HIDiC. In the PP-HIDiC it can be possible that some channels in the packing get very little or even no liquid. For this kind of very severe maldistribution, another method is needed.

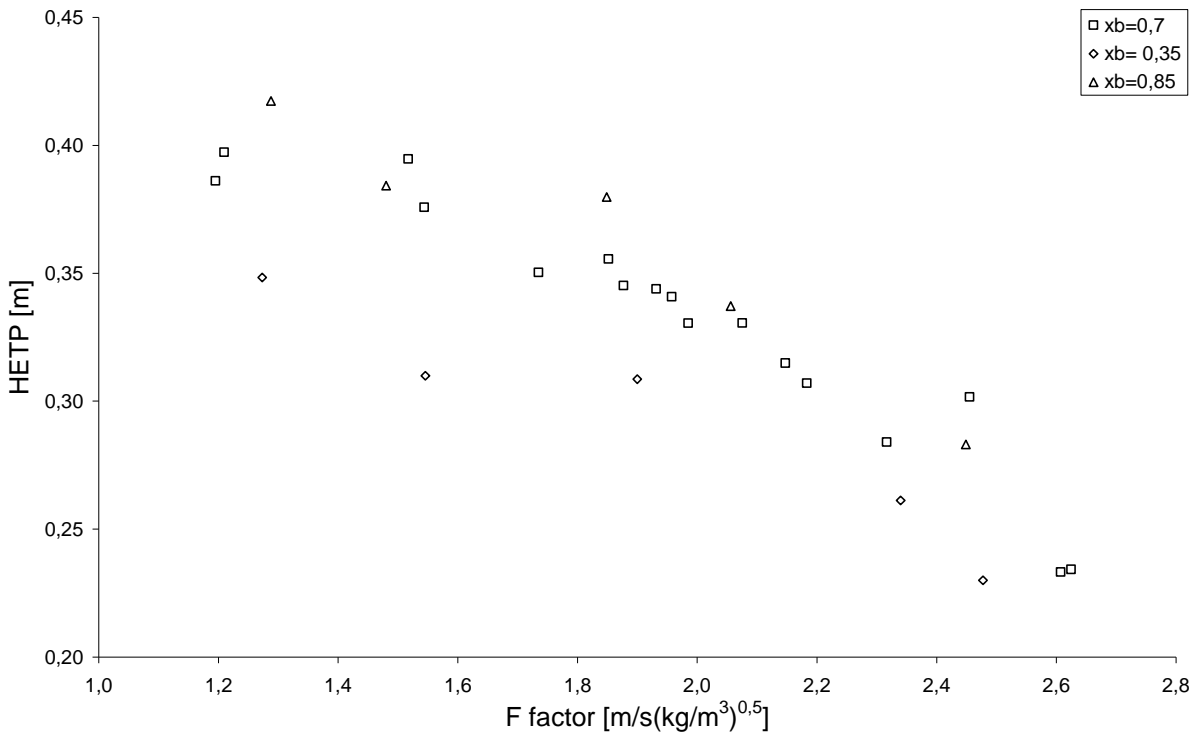


Figure 22 Effect of feed composition on the efficiency of the PP-HIDiC

Another approach to indicate maldistribution is by using the Delft model. Figure 15 shows the HiDiC column should have a much lower HETP than observed. The column has a specific geometric surface area of $614 \text{ m}^2/\text{m}^3$, but, according to the model, functions as a column which has a specific surface area $170 \text{ m}^2/\text{m}^3$. Due to channelling of liquid and probably unused channels in the packing material only 28% of the surface area installed in the column is used.

There are different factors which influence the use of the surface area in the column.

First, as stated earlier, the open sides of channels in the packing material are closed off by the sheet placed between the elements. A large part of the liquid now collects in the lowest corner of the triangular channels, flowing as a rivulet and leaving a relatively large fraction of surface area in the channel unused.

Due to the inserted sheet there are no contact points of crossing channels where in a conventional packed bed liquid tends to mix with liquid flowing through a neighbouring channel in opposite direction. This small scale mixing occurring at many contact points along a channel is responsible for maintaining the concentration gradient within the height of a packing element, while the large scale mixing occurs at transitions between subsequent packing elements. Both effects are greatly reduced (some limited communication is possible through perforations) by inserted plate. The latter however largely increases the installed area but effectively, due to absence of any means to reduce liquid maldistribution, the overall performance is well below that expected. This however may mean that the same packing but without the perforated plate could perform better.

5. Conclusions

5.1 Mass transfer

In comparison with the PF-HiDiC mass transfer in the PP-HiDiC has improved by a factor 4. A typical HETP for the PP-HiDiC is 33 cm. At higher F-factors mass transfer is better. Measurements are done until an F-factor of about $2.6 \text{ Pa}^{0.5}$ because the capacity of the reflux pump was limiting. Mass transfer kept getting better until this maximum F-factor. Heat transfer in the PP-HiDiC did have an effect on mass transfer, but the effect was small and the average separation of the stripping mode and the rectification mode was similar to the separation found in adiabatic operation. In stripping mode the mass transfer is better than in rectifying mode. This means to some extent heat can be subtracted or added to the column without influencing the mass transfer in the whole column. In the design of a HiDiC column, it can be wise to take into account that HETP in the stripping section is higher than in the rectification section.

5.2 Pressure drop

The pressure drop shows a trend as expected from a packed column. In the preloading regime pressure drop rises slowly, while after the loading point it increases faster with increasing F-Factor. The Delft model shows a lower pressure drop in the preloading regime. In comparison with a normal distillation column the HiDiC column contains a lot of channels which end at the column wall, which increases pressure drop. In diabatic measurements the pressure drop as a function of the average F-factor seems to have a similar trend as the adiabatic pressure drop.

5.3 Heat transfer

In the PP-HiDiC heat was transferred from or to the thermal bath fluid. The average UA value in this case was 335 W/K. With a total wall area of 0.4 m^2 the overall heat transfer coefficient U will be $844 \text{ W/m}^2\text{K}$.

5.4 Maldistribution

Maldistribution has not been demonstrated by the method of Billingham¹⁵, probably because this method is designed for large scale columns with relatively low maldistribution.

The Delft model shows that the column operates as a column with a specific surface area of $170 \text{ m}^2/\text{m}^3$ while $614 \text{ m}^2/\text{m}^3$ is installed. This shows that about 28% of the surface area is used. Because a metal sheet is installed between the packing plates, triangular channels are formed. The liquid now collects in the corners of these channels leaving parts of the surface area unused. In the HiDiC column a lot of these triangular channels end at the column wall, which makes it difficult for both liquid and gas to enter these channels.

All of this taken into account, it seems likely that there is a severe liquid maldistribution in the PP-HiDiC. In the design of a next experimental setup liquid distribution over the column cross sectional area is an important factor.

6. Recommendations

The PP HIDiC has a perforated plate placed between the packing sheets. This plate closes off channels in the packing and therefore eliminates mixing of gas and liquid from different channels.

A packed column without a perforated plate could give a better separation, as found by Olujić et al.²³. It should be noted that the packing elements then need to be in direct contact. When another PP HIDiC is designed, this can be taken into account.

A very good liquid distribution over the column cross sectional area is needed to use all installed surface area in the column. Both initial liquid distribution and redistribution in the column are important in the design of a next experimental setup.

In the PF-HIDiC and PP-HIDiC test setup heat is transferred between the thermal bath fluid side and the distillation side of the column. In order to test the HIDiC principle properly, in a next test setup a rectification section and a stripping section can be placed next to each other. Each section can be operated at a different pressure and with its own condenser and reboiler. With such an experimental setup the actual heat transfer between a rectifying section and a stripping section of a HIDiC and all effects on the column can be measured and analyzed.

It is important that a good overview of the internals of the column is present. Especially for modelling the column, details of the internals are needed. When building a new HIDiC column it is wise to take pictures and document details about the internals before the column is put together.

Measurements above an F-factor of $2.6 \text{ Pa}^{0.5}$ were not possible because the flow of the reflux pump was limiting. At an F-factor of $2.6 \text{ Pa}^{0.5}$ the flooding point was not yet reached, so the HIDiC can have a higher capacity than measured.

The flooding point in a normal packed column is around an F-factor of $2 \text{ Pa}^{0.5}$ to $2.5 \text{ Pa}^{0.5}$ so when the flooding point is only a bit higher, the capacity of the reflux pump limits the measurements. A larger reflux pump is needed to enable reaching the flood point, i.e. maximum load achievable with the PP-HIDiC.

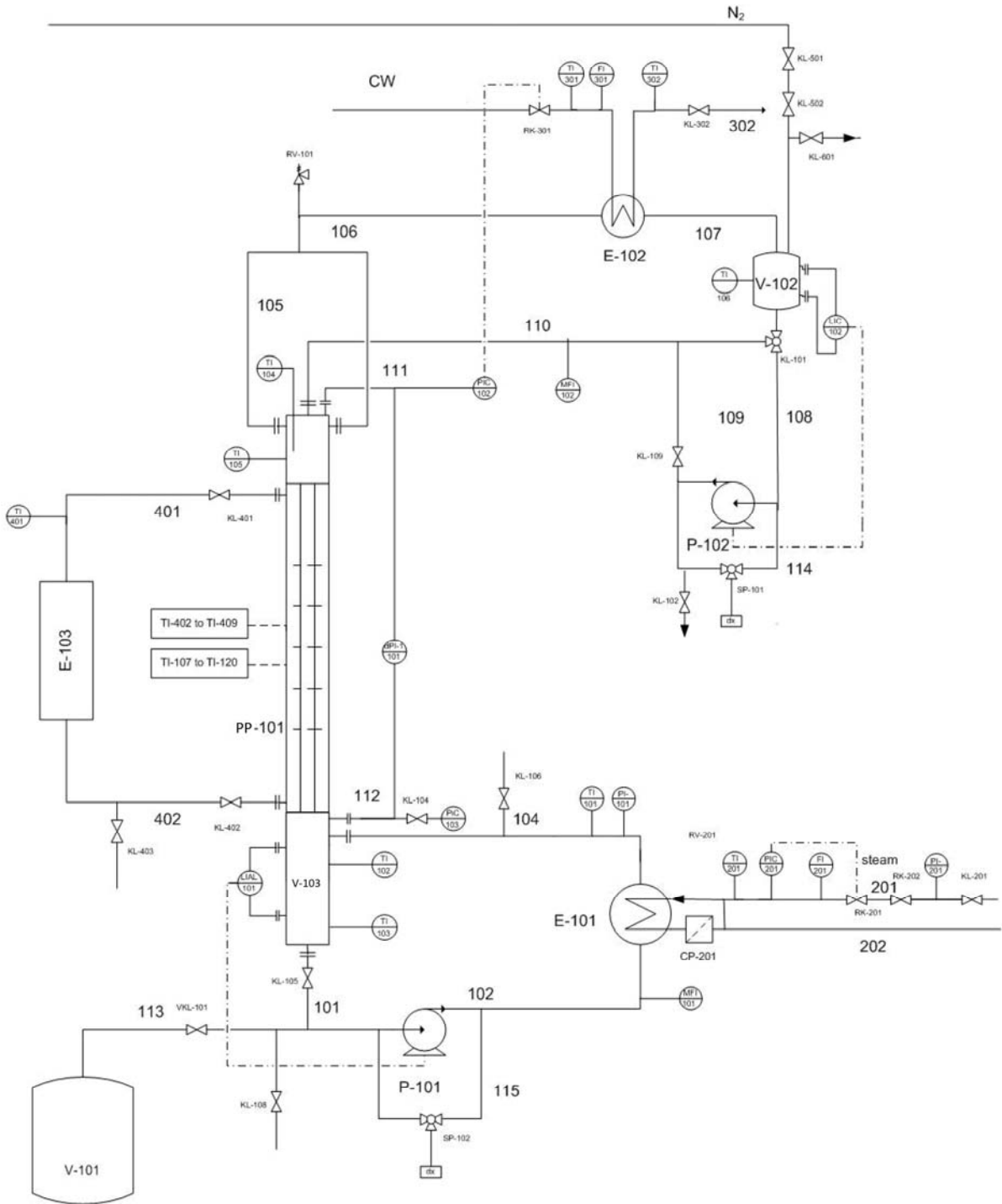
Due to fluctuations in the steam supply network, the reboiler duty fluctuated to certain extent. This causes fluctuations in the whole column. For example, the trend found in the steam flow through the reboiler was also visible in the pressure of the column and in the reflux with some delay. Steam has caused more problems due to hammering, a defect valve and a rotten pipe. To get a more stable column, it can be better to install an electrically heated reboiler.

References

-
- ¹ Seader J.D. and Henley E.J., Separation Process Principles. Second edition. Wiley, Hoboken, NJ (2006)
- ² Strathern, P., Mendeleev's Dream - The Quest For the Elements. Berkley Books New York (2000)
- ³ Ridgway, H.F., Sheets Advanced Membrane Technology, Stanford University 7 may 2008 available: <http://www.stanford.edu/group/ees/rows/presentations/Ridgway.pdf>
- ⁴ ter Horst, J. MST Scheidingstechnologie- History of Distillation. Lecture slides Scheidingstechnologie 2008/1009 TU Delft
- ⁵ Hugill, J.A., van Dorst E.M., Design of a heat-integrated distillation column based on a plate-fin heat exchanger ECN-RX--05-157 (2005)
- ⁶ Palivachi P.A., Systems modelling as a design tool for energy efficiency research within the European Union, Computational Chemical Engineering, Vol 20, page 467-472, 1996
- ⁷ Mah, R.S., Nicholas, J.J. and Wodnik, R.B., Distillation with Secondary Reflux and Vaporization, a comparative evaluation, AIChE J, 23, 651-658 (1977)
- ⁸ Aso, K., Takamatsu, T. and Nakaiwa, M., Heat Integrated Distillation Column, U.S. Patent 5,873,047 (1998)
- ⁹ Nakaiwa, M., Huang, K., Naito, K., Endo, A., Akiya, T., Nakane, T. and Takamatsu, T., Parameter analysis and optimization of ideal heat-integrated distillation columns, Computers and Chemical Engineering, 25, 737-744 (2001)
- ¹⁰ Olujić, Ž., Fakhri, F., de Rijke, A., de Graauw, J. and Jansens, P.J., Internal heat integration – the key to an energy conserving distillation column, J. Chem. Tech. Biotech., 78, 241-248 (2003)
- ¹¹ Hugill, J.A. and van Dorst, E.M., The use of compact heat exchangers in heat-integrated distillation columns, 5th Int. Conf. on Enhanced, Compact and Ultra-Compact Heat Exchangers, September 2005, Hoboken, USA, 310-317 (2005)
- ¹² Bardow, A., ter Horst, J. and Lubary, M., Separation Process Design and Operation- Distillation-Column Design. Lecture slides SPDO 2009/2010 TU Delft
- ¹³ Olujić, Ž., Behrens, M., Colli, L., and Paglianti, A., Predicting the Efficiency of Corrugated Sheet Structured Packings with Large Specific Surface Area. Chem. Biochem. Eng. Q 18 (2) 89-96 (2004)
- ¹⁴ Van den Akker H.E.A and Mudde R.F. Fysische Transportverschijnselen I. DUP Blue Print, Delft, 2003

-
- ¹⁵ Billingham, J. F., Lockett M. J., A simple method to assess the sensitivity of packed distillation columns to maldistribution, *Trans IChemE*, vol 80, Part A, 373-382 (2002)
- ¹⁶ Strijker, M., Msc thesis: Heat integrated distillation in a plate-fin heat exchanger: Partial validation of predictive models, Delft University of Technology, Delft (2009)
- ¹⁷ Gmehling, J.G., Onken, U. and Arlt, W., Vapour Liquid Equilibrium Data Collection, *Chemistry Data Series Vol.1 part 6a* pp 300, 303, 304
- ¹⁸ Sieg, L., *Chem. Ing. Tech.* 22, 322 (1950)
- ¹⁹ Colonna, P., van der Stelt, T.P., FluidProp: a program for the estimation of thermo physical properties of fluids, Energy Technology Section, Delft University of Technology, The Netherlands, 2004, (<http://www.FluidProp.com>)
- ²⁰ Malhotra, A., Bsc thesis: Heat integrated distillation in a plate fin heat exchanger, Delft University of Technology, Delft (2010)
- ²¹ Olujić, Ž., Seibert, A.F. and Fair, J.R., Influence of corrugation geometry on the performance of structured packings: an experimental study, *Chemical Engineering and Processing* 39, 335-342 (1999)
- ²² Fair, J. R., Frank Seibert, A., Behrens, M., Saraber, P. P. and Olujić, Ž., Structured packing performance- experimental evaluation of two predictive models, *Ind. Eng. Chem. Res.* 39, 1788-1796 (2000)
- ²³ Olujić, Ž., Jansen, H., Kaibel, B., Rietfort, T. and Zich, E., Stretching the Capacity of Structured Packings, *Ind. Eng. Chem. Res.* 40, 6172-6180 (2001)
- ²⁴ Behrens, M., Olujić, Ž. and Jansens, P.J., Liquid Flow behavior in Catalyst Containing Pockets of Modular Catalytic Structured Packing Katapak SP *Ind. Eng. Chem. Res.* 46, 3884-3890 (2007)

A: P&ID



Equipment List			
Tag	Description	Tag	Description
E-101	Reboiler	P-102	Reflux pump
E-102	Condenser	V-101	Safety storage vessel
E-103	Thermostatic bath	V-102	Reflux buffer vessel
P-101	Reboiler pump	V-103	Reboiler buffer vessel

B. Experimental Data

	Measurement date	measurement	F-factor	delta F	delta T (°C)	T column	T reflux	Xmolar b	Xmolar t	$C_{H_2O,reflux}$	N fenske	N rebollet	N actual	HETP (M)	delta P (mbar)	MF102.1 (kg/hr)	internal reflux	delta mass flow (kg/hr)	heat transferred (W)	UA
cyclohexane	13-okt	1	1.52		adiabatic	84,1836	60,39	0,7436	0,9252	1,549	3,31	0,76	2,63	0,39	1,87	25,31	29,01	0	0	
heptane		2	1,34	-0,176561	-1,38	82,80	61,41	0,7459	0,9277	1,555	3,34	0,82	2,62	0,40	1,49	22,66	25,64	3,38	331	240,0361
cyclohexane		3	1,15	-0,370757	-2,42	81,76	60,25	0,7453	0,9299	1,560	3,42	0,83	2,59	0,39	1,31	19,37	21,92	7,09	696	-287,232
heptane	14-okt	1	2,32		adiabatic	83,96536	68,36	0,7259	0,9429	1,551	4,17	0,65	3,52	0,28	5,94	40,43	44,30	0,00	0	
cyclohexane		2	2,09	-0,224193	-1,25	82,74	68,24	0,7369	0,9387	1,556	3,85	0,66	3,19	0,31	4,82	36,75	40,01	4,29	421	-337,1195
heptane		3	1,92	-0,396902	-2,16	81,83	68,23	0,7364	0,9357	1,560	3,71	0,66	3,05	0,33	4,37	33,89	36,71	7,59	745	-944,9327
cyclohexane	15-okt	1	1,21		adiabatic	83,96834	65,08	0,7451	0,9261	1,546	3,34	0,82	2,62	0,40	1,13	20,72	23,13	0,00	0	
heptane		2	1,08	-0,12	-1,14	82,83	64,97	0,7406	0,9278	1,555	3,29	0,84	2,45	0,41	1,03	18,69	20,74	2,39	234	205,636
cyclohexane	20-10-2010	1	1,88		adiabatic	83,88	66,16	0,7351	0,9313	1,551	3,62	0,72	2,90	0,35	2,77	32,73	35,89	0,00	0	
heptane		2	1,74	-0,14	-0,92	82,96	68,10	0,7414	0,9331	1,555	3,58	0,74	2,84	0,35	2,61	30,45	33,23	2,66	261	-282,3785
cyclohexane		3	1,52	-0,36	-1,99	81,89	67,65	0,7421	0,9304	1,559	3,46	0,77	2,69	0,37	2,26	26,75	29,09	6,79	667	-335,0928
heptane	21-10-2010	1	2,62		adiabatic	84,18	69,47	0,7132	0,9544	1,552	4,85	0,56	4,27	0,23	9,39	46,06	50,18	0,00	0	
cyclohexane		2	2,47	-0,16	-1,15	83,03	69,63	0,7137	0,9512	1,556	4,65	0,56	4,09	0,24	8,42	43,60	47,17	3,01	296	-258,7306
heptane		3	2,25	-0,37	-2,20	81,98	69,69	0,7189	0,9478	1,561	4,40	0,62	3,78	0,26	7,24	40,05	43,06	7,13	701	-318,4637
cyclohexane	22-10-2010	1	2,182939		adiabatic	84,23914	68,19	0,7169	0,9332	1,550	3,90	0,64	3,26	0,31	5,09	38,00	41,74	0	0	
heptane								0,2831	0,0668											

	Measurement date	measurement	F-factor	della F	della T (°C)	T column	T reflux	Xmolar b	Xmolar t	α_{liquid}	N fenske	N reboiler	N actual	HETP (M)	della P (mbar)	M/F021 (kg/hr)	Internal reflux	della mass flow (kg/hr)	heat transferred (W)	U
cyclohexane	26-ott	1	1,20		adiabatic	84,45	60,86	0,7422	0,9266	1,548	3,36	0,794	2,69	0,366	1,08	19,96	22,85	0	0	
heptane		2	1,49	0,29	1,50	85,95	62,50	0,2578	0,0734	1,542	3,46	0,780	2,68	0,373	1,36	24,89	28,48	5,62	552	368,4284
cyclohexane								0,2686	0,0746											
heptane	28-ott	1	2,15		adiabatic	84,03	67,88	0,7280	0,0931	1,551	3,84	0,862	3,18	0,315	4,20	37,36	41,06	0	0	
cyclohexane		2	2,55	0,41	1,48	85,51	68,02	0,7275	0,0936	1,544	3,86	0,578	3,28	0,305	5,92	44,08	48,81	7,75	761	513,9047
heptane								0,2725	0,0654											
cyclohexane		3	2,64	0,49	1,99	86,02	67,77	0,7294	0,0947	1,543	4,44	0,591	3,85	0,280	5,91	45,42	50,48	9,42	927	465,6235
heptane	29-ott	1	1,73		adiabatic	83,89	68,27	0,7264	0,0927	1,551	3,59	0,736	2,85	0,350	2,33	30,27	33,17	0	0	
cyclohexane		2	2,07	0,34	1,58	85,47	67,82	0,7306	0,0926	1,544	3,54	0,868	2,87	0,348	3,04	35,74	39,62	6,44	632	399,855
heptane		3	2,14	0,41	1,97	85,868071515	68,34	0,7333	0,0934	1,542	3,46	0,807	2,85	0,350	3,33	36,95	40,93	7,76	761	386,1117
cyclohexane								0,2687	0,0751											
heptane	1-11-2010	1	2,08		adiabatic	84,12	72,50	0,7261	0,0924	1,550	3,66	0,632	3,03	0,331	3,95	37,04	39,68	0	0	
cyclohexane								0,2739	0,0706											
heptane	2-11-2010	1	2,46		adiabatic	83,87	68,84	0,7115	0,0927	1,552	4,32	0,558	3,32	0,302	7,45	43,00	46,95	0,00	0	
cyclohexane								0,2885	0,0573											
heptane	measurement of 2 hours	2	3,34	0,88	1,77	85,64	67,33	0,6960	0,0952	1,546	5,12	0,426	4,70	0,213	8,38	57,40	63,81	16,86	1659	937,0743
cyclohexane								0,3040	0,0448											
heptane	4-11-2010	1	1,543739		adiabatic	84,33636633	61,68	0,7282	0,0927	1,549	3,42	0,757	2,86	0,376	1,71	25,91	29,52	0	0	
cyclohexane		2	1,804884	0,26	1,192506321	85,52867265	62,80	0,7308	0,0773	1,544	3,41	0,897	2,72	0,368	2,03	30,28	34,51	4,99	490	410,5625
heptane		3	1,861783	0,32	1,637	85,97342545	63,21	0,7269	0,0925	1,542	3,46	0,714	2,75	0,364	2,13	31,23	35,60	6,08	596	364,2399
cyclohexane		1	2,607315		adiabatic	83,93734266	67,14	0,6891	0,0945	1,553	4,81	0,522	4,29	0,283	9,68	45,22	49,86	0	0	
heptane	5-nov							0,3109	0,0515											
cyclohexane		1	1,851625		adiabatic	83,11032111	68,29	0,7158	0,0916	1,554	3,49	0,883	2,81	0,356	2,64	32,45	35,41	0	0	
heptane	9-nov							0,2842	0,0784											
cyclohexane		2	2,211889	0,36	2,28	85,39154543	68,05	0,7143	0,0915	1,544	3,56	0,569	2,99	0,335	3,46	38,22	42,30	6,89	675	296,2004
heptane		3	2,265728	0,41	2,73	85,84280326	67,89	0,7089	0,0930	1,543	3,68	0,827	3,05	0,328	3,60	38,02	43,33	7,92	776	284,3912
cyclohexane								0,2811	0,0770											
heptane	10-nov							0,7179	0,0922	1,552	3,50	0,593	2,91	0,344	2,91	33,80	36,93	0	0	
cyclohexane		= 80 kg/h	1,931221		adiabatic	83,6532375	68,59	0,2821	0,0778	1,551	3,38	0,451	2,93	0,341	3,03	34,11	37,43	0,00	0	
heptane		= 60 kg/h	1,95719		adiabatic	83,80422971	68,01	0,2812	0,0814	1,549	3,19	0,164	3,03	0,331	3,19	34,59	37,86	0	0	
cyclohexane		= 40 kg/h	1,985042		adiabatic	84,13235456	68,34	0,2810	0,0882											

F-factor	delta F	T	T reflux	Xmolar b	Xmolar t	α_{Margules}	N fenske	Nreboiler	N actual	HETP (M)	delta P (mbar)	MF1021 (kg/hr)
1,29		82,42	70,26	0,846625	0,96	1,559	3,18	0,784	2,40	0,417	1,29	22,92
				0,1534	0,0423							
1,85		82,48	71,60	0,844503	0,96	1,559	3,30	0,664	2,63	0,380	2,67	33,15
				0,1555	0,0409							
2,45		82,36	74,17	0,829308	0,97	1,560	4,08	0,548	3,53	0,283	7,57	44,60
				0,1707	0,0325							
2,055812		82,44	73,14	0,832904	0,96	1,559	3,59	0,626	2,97	0,337	3,71	37,21
				0,1671	0,0391							
1,48		82,43	72,08	0,84	0,96	1,559	3,37	0,765	2,60	0,384	1,69	26,62
				0,1605	0,0411							
2,48		88,26	72,36	0,321514	0,81	1,572	4,87	0,517	4,35	0,230	8,03	43,04
				0,6785	0,1892							
1,55		88,35	71,40	0,35	0,76	1,566	3,93	0,700	3,23	0,310	1,72	26,66
				0,6451	0,2382							
1,90		88,65279251	67,75	0,35	0,752352	1,566	3,89	0,645	3,24	0,309	2,79	32,03
				0,6528	0,2476							
2,34		88,41	67,16	0,33	0,779222	1,570	4,38	0,552	3,83	0,261	6,15	39,40
				0,6716	0,2208							
1,27		88,43	65,43	0,352381	0,755356	1,566	3,87	0,746	2,87	0,348	1,22	21,21
				0,6476	0,2446							

C. Relative volatility

Meting		xb	xt	T1	Psat ch	Psat nh	gamma ch	gamma nh	$\alpha_{Margules}$	$\alpha_{average}$
13-okt	1	0,744	0,925	84,2	0,843	0,491	0,989	0,910	1,546	1,549
		0,256	0,075		0,843	0,491	0,999	0,905	1,553	
		0,746	0,928		82,8	0,809	0,469	0,989	0,910	
	2	0,254	0,072		0,809	0,469	0,999	0,905	1,559	
		0,743	0,930	81,8	0,784	0,454	0,989	0,910	1,556	1,560
		0,257	0,070		0,784	0,454	0,999	0,905	1,564	
14-okt	1	0,726	0,943	84,0	0,838	0,488	0,988	0,911	1,547	1,551
		0,274	0,057		0,838	0,488	0,999	0,906	1,556	
		0,736	0,939	82,7	0,807	0,468	0,989	0,911	1,552	1,556
	2	0,264	0,061		0,807	0,468	0,999	0,906	1,561	
		0,736	0,936	81,8	0,786	0,455	0,989	0,910	1,556	1,560
		0,264	0,064		0,786	0,455	0,999	0,906	1,564	
15-okt	1	0,745	0,926	84,0	0,837	0,487	0,989	0,910	1,546	1,550
		0,255	0,074		0,837	0,487	0,999	0,905	1,554	
		0,750	0,928	82,8	0,810	0,470	0,989	0,909	1,551	1,555
	2	0,250	0,072		0,810	0,470	0,999	0,905	1,559	
		0,735	0,931	83,9	0,835	0,486	0,989	0,911	1,547	1,551
		0,265	0,069		0,835	0,486	0,999	0,906	1,555	
	2	0,741	0,933	83,0	0,813	0,472	0,989	0,910	1,551	1,555
		0,259	0,067		0,813	0,472	0,999	0,906	1,559	
		0,742	0,930	81,9	0,787	0,456	0,989	0,910	1,555	1,559
	3	0,258	0,070		0,787	0,456	0,999	0,905	1,563	
		0,713	0,954	84,2	0,843	0,491	0,987	0,913	1,547	1,552
		0,287	0,046		0,843	0,491	1,000	0,907	1,556	
21-10-2010	1	0,714	0,951	83,0	0,815	0,473	0,987	0,913	1,552	1,556
		0,286	0,049		0,815	0,473	0,999	0,907	1,561	
		0,719	0,948	82,0	0,789	0,457	0,987	0,912	1,556	1,561
	3	0,281	0,052		0,789	0,457	0,999	0,906	1,565	
		0,717	0,933	84,2	0,844	0,492	0,987	0,912	1,546	1,550
		0,283	0,067	85,0	0,844	0,492	0,999	0,906	1,553	
26-okt	1	0,742	0,927	84,5	0,849	0,495	0,989	0,910	1,544	1,548
		0,258	0,073		0,849	0,495	0,999	0,905	1,552	
		0,734	0,925	86,0	0,887	0,519	0,988	0,911	1,538	1,542
	2	0,266	0,075		0,887	0,519	0,999	0,905	1,545	
		0,728	0,935	84,0	0,839	0,488	0,988	0,911	1,547	1,551
		0,272	0,065		0,839	0,488	0,999	0,906	1,555	
	2	0,727	0,935	85,5	0,876	0,512	0,988	0,911	1,541	1,544
		0,273	0,065		0,876	0,512	0,999	0,906	1,548	
		0,729	0,949	86,0	0,889	0,520	0,988	0,911	1,538	1,543
	3	0,271	0,051		0,889	0,520	0,999	0,906	1,548	
		0,726	0,928	83,9	0,836	0,486	0,988	0,911	1,547	1,551
		0,274	0,072		0,836	0,486	0,999	0,905	1,554	
	2	0,731	0,927	85,5	0,875	0,511	0,988	0,911	1,541	1,544
		0,269	0,073		0,875	0,511	0,999	0,905	1,547	
		0,733	0,925	85,9	0,885	0,518	0,988	0,911	1,539	1,542
	3	0,267	0,075		0,885	0,518	0,999	0,905	1,546	
		0,726	0,929	84,1	0,841	0,490	0,988	0,911	1,546	1,550
		0,274	0,071		0,841	0,490	0,999	0,905	1,553	
2-11-2010	1	0,712	0,943	83,9	0,835	0,486	0,987	0,913	1,548	1,552
		0,288	0,057		0,835	0,486	0,999	0,906	1,556	
		0,696	0,955	85,6	0,879	0,514	0,986	0,914	1,542	1,546
4-11-2010	1	0,304	0,045		0,879	0,514	1,000	0,907	1,550	
		0,728	0,923	84,3	0,847	0,493	0,988	0,911	1,545	1,549
		0,272	0,077		0,847	0,493	0,999	0,905	1,552	
	2	0,731	0,923	85,5	0,877	0,512	0,988	0,911	1,540	1,544
		0,269	0,077		0,877	0,512	0,999	0,905	1,547	
		0,727	0,923	86,0	0,888	0,520	0,988	0,911	1,539	1,542
	3	0,273	0,077		0,888	0,520	0,999	0,905	1,545	
		0,689	0,948	83,9	0,837	0,487	0,986	0,915	1,550	1,553
		0,311	0,052		0,837	0,487	0,999	0,906	1,557	
9-nov	1	0,716	0,922	83,1	0,816	0,474	0,987	0,912	1,551	1,554
		0,284	0,078		0,816	0,474	0,999	0,905	1,557	
		0,714	0,921	85,4	0,873	0,510	0,987	0,912	1,542	1,544
	2	0,286	0,079		0,873	0,510	0,999	0,905	1,547	
		0,709	0,923	85,8	0,885	0,517	0,987	0,913	1,540	1,543
		0,291	0,077		0,885	0,517	0,999	0,905	1,545	
10-nov	ML 80 kg/h	0,718	0,922	83,7	0,830	0,482	0,987	0,912	1,549	1,552
		0,282	0,078		0,830	0,482	0,999	0,905	1,555	
		0,719	0,919	83,8	0,833	0,485	0,987	0,912	1,548	1,551
	ML 60 kg/h	0,281	0,081		0,833	0,485	0,999	0,905	1,554	
		0,719	0,912	84,1	0,841	0,490	0,987	0,912	1,547	1,549
		0,281	0,088		0,841	0,490	0,998	0,905	1,551	
23-nov	1	0,847	0,958	82,4	0,800	0,463	0,995	0,905	1,554	1,559
		0,153	0,042		0,800	0,463	1,000	0,907	1,564	
		0,845	0,959	82,5	0,801	0,464	0,995	0,905	1,554	1,559
	2	0,155	0,041		0,801	0,464	1,000	0,907	1,564	
		0,829	0,968	82,4	0,798	0,463	0,994	0,905	1,553	1,560
		0,171	0,032		0,798	0,463	1,000	0,908	1,566	
	2	0,833	0,961	82,4	0,800	0,464	0,995	0,905	1,553	1,559
		0,167	0,039		0,800	0,464	1,000	0,907	1,565	
		0,839	0,959	82,4	0,800	0,464	0,995	0,905	1,554	1,559
	3	0,161	0,041		0,800	0,464	1,000	0,907	1,565	
		0,322	0,811	88,3	0,948	0,558	0,982	0,970	1,617	1,572
		0,678	0,189		0,948	0,558	0,993	0,906	1,528	
25-nov	1	0,355	0,762	88,3	0,951	0,560	0,979	0,964	1,604	1,566
		0,645	0,238		0,951	0,560	0,990	0,909	1,528	
		0,347	0,752	88,7	0,959	0,565	0,980	0,966	1,605	1,566
26-11-2010	1	0,653	0,248		0,959	0,565	0,990	0,909	1,527	
		0,328	0,779	88,4	0,953	0,561	0,981	0,969	1,613	1,570
		0,672	0,221		0,953	0,561	0,991	0,907	1,527	
	3	0,352	0,755	88,4	0,953	0,562	0,979	0,965	1,604	1,566
		0,648	0,245		0,953	0,562	0,990	0,909	1,527	

D. Reboiler stages

PP hidic measured values adiabatic

date	Fr/F	ML	MV	xb	alfa	xr1	xr2	yr1	yr2	Nreboiler
13-okt	0,241047619	105	25,31	0,74	1,549102	0,063	0,721	0,095	0,800067	0,779
14-okt	0,376514445	107,3	40,4	0,725	1,551391	0,134	0,693	0,194	0,777914	0,647
15-okt	0,193638915	106,9	20,7	0,745	1,546374	0,046	0,730	0,070	0,807061	0,823
20-okt	0,303055556	108	32,73	0,735	1,55091	0,091	0,710	0,134	0,791785	0,719
21-okt	0,444594595	103,6	46,06	0,713	1,551669	0,190	0,674	0,267	0,762106	0,579
22-okt	0,383838384	99	38	0,717	1,549935	0,143	0,684	0,206	0,770239	0,639
26-okt	0,224382022	89	19,97	0,742	1,548065	0,057	0,724	0,086	0,802744	0,794
28-okt	0,36131528	103,4	37,36	0,728	1,550662	0,124	0,698	0,179	0,781592	0,662
29-okt	0,285176471	106,25	30,3	0,726	1,55084	0,086	0,702	0,127	0,785357	0,736
1-nov	0,39154334	94,6	37,04	0,726	1,549972	0,143	0,693	0,206	0,777568	0,632
2-nov	0,462365591	93	43	0,711	1,468882	0,212	0,675	0,284	0,753018	0,558
4-nov	0,263206014	98,44	25,91	0,728	1,548625	0,076	0,706	0,112	0,788417	0,757
5-nov	0,499116998	90,6	45,22	0,689	1,553133	0,263	0,642	0,357	0,735976	0,522
9-nov	0,339114083	95,72	32,46	0,716	1,554149	0,116	0,687	0,170	0,773071	0,683
10-nov	0,431122449	78,4	33,8	0,718	1,55178	0,176	0,680	0,249	0,767628	0,593
10-nov	0,572315436	59,6	34,11	0,719	1,550912	0,325	0,668	0,427	0,757206	0,451
10-nov	0,847794118	40,8	34,59	0,719	1,54914	1,486	0,640	1,268	0,733259	0,164

diabatic

measurement	Fr	F	xb	alfa	xr1	xr2	yr1	yr2	Nreboiler	
13-okt	2	114,46	22,66	0,746	1,555147	0,047	0,731	0,072	0,808345	0,820
	3	105,56	19,37	0,743	1,559867	0,043	0,729	0,066	0,80721	0,833
14-okt	2	101,46	36,75	0,736	1,556285	0,120	0,706	0,175	0,78888	0,662
	3	93,45	33,89	0,736	1,560069	0,120	0,706	0,175	0,789126	0,662
15-okt	2	108,32	18,69	0,749	1,54974	0,039	0,736	0,060	0,81239	0,843
20-okt	2	108,31	30,45	0,741	1,554876	0,079	0,718	0,117	0,79869	0,741
	3	106,71	26,75	0,742	1,559344	0,066	0,722	0,100	0,801933	0,770
21-okt	2	93,09	43,6	0,714	1,556369	0,210	0,672	0,293	0,761434	0,555
	3	99,75	40,05	0,719	1,560584	0,153	0,684	0,220	0,771438	0,622
26-okt	2	104,16	24,89	0,734	1,541802	0,065	0,715	0,096	0,794565	0,780
28-okt	2	98,71	44,08	0,729	1,544351	0,181	0,691	0,254	0,775712	0,578
	3	104,83	45,42	0,727	1,543043	0,172	0,690	0,243	0,774842	0,591
29-okt	2	100,62	35,74	0,731	1,543972	0,119	0,702	0,172	0,784133	0,668
	3	88,49	36,95	0,733	1,542154	0,157	0,698	0,223	0,781244	0,607
2-nov	2	96,6	57,4	0,696	1,546091	0,390	0,641	0,497	0,733794	0,426
4-nov	2	95,83	31,23	0,731	1,543512	0,103	0,704	0,151	0,786178	0,697
	3	98,65	30,28	0,727	1,541726	0,096	0,702	0,140	0,783931	0,714
9-nov	2	84,11	38,22	0,714	1,544444	0,198	0,674	0,277	0,761723	0,569
	3	98,79	39,02	0,709	1,542792	0,156	0,675	0,221	0,761773	0,627

xb = 0.9

measurement	Fr	F	xb	alfa	xr1	xr2	yr1	yr2	Nreboiler	
23-nov	1	94,16454	22,92203	0,846625	1,559194	0,036	0,834	0,056	0,886619	0,784
	2	89,19208	33,15185	0,844503	1,558975	0,071	0,824	0,107	0,879398	0,664
24-nov	1	91,35863	44,60278	0,829308	1,559796	0,133	0,799	0,192	0,861102	0,548
	2	90,82863	37,2061	0,832904	1,559039	0,092	0,808	0,136	0,868099	0,626
	3	101,0833	26,62424	0,839445	1,559055	0,043	0,825	0,065	0,880155	0,765

xb = 0.5

measurement	Fr	F	xb	alfa	xr1	xr2	yr1	yr2	Nreboiler	
25-nov	1	93,01629	43,04198	0,321514	1,572428	0,539	0,276	0,647	0,374567	0,517
	2	92,61407	26,66334	0,354858	1,565725	0,231	0,325	0,319	0,429482	0,700
26-nov	1	94,04018	32,02669	0,347234	1,565953	0,302	0,312	0,404	0,415328	0,645
	2	91,79818	39,40284	0,328379	1,570332	0,462	0,285	0,574	0,385479	0,552
	3	87,32007	21,21416	0,352381	1,56589	0,182	0,327	0,259	0,431927	0,746